Title:

Dual-specific autophosphorylation of kinase IKK2 enables phosphorylation of substrate IκBα through a phosphoenzyme intermediate

Prateeka Borar[1], Tapan Biswas[2,#], Ankur Chaudhuri[3,4#], Pallavi Rao T[4,5], Swasti Raychaudhuri[4,5], Tom Huxford[6], Saikat Chakrabarti[3,4] Gourisankar Ghosh[2] & Smarajit Polley[1,*]

[1]Department of Biological Sciences, Bose Institute, Kolkata 700091, India; [2]Department of Chemistry and Biochemistry, University of California San Diego, La Jolla, CA 92093, USA; [3]Structural Biology and Bioinformatics Division, CSIR-Indian Institute of Chemical Biology, Kolkata 700032, India; [4]Academy of Scientific and Innovative Research (AcSIR), Ghaziabad 201002, India, [5]CSIR-Centre for Cellular and Molecular Biology, Uppal Road, Hyderabad 500007, India; [6]Department of Chemistry and Biochemistry, San Diego State University, San Diego, CA 92182, USA.

*Correspondence to be addressed to: spolley@jcbose.ac.in, smarajit.polley@gmail.com

[#] These two authors have contributed equally to this work.

Abstract:

Rapid and high-fidelity phosphorylation of serine residues at positions 32 and 36 of IκBα by IKK2, a prototypical Ser/Thr kinase, is critical for canonical NF-κB activation. Here, we report that IKK2 not only phosphorylates substrate serine residues and autophosphorylates its own activation loop, but also autophosphorylates at a tyrosine residue proximal to the active site and is, therefore, a dual-specificity kinase. We observed that mutation of Y169, an autophosphorylatable tyrosine located at the DFG+1 (DLG in IKK1) position, to phenylalanine renders IKK2 incapable of catalyzing phosphorylation at S32 within its IκBα substrate. We also observed that mutation of the phylogenetically conserved ATP-contacting residue K44 in IKK2 to methionine converts IKK2 to an enzyme that no longer catalyzes specific phosphorylation of IκBα at S32 or S36, but rather directs phosphorylation of IκBα at other residues. Lastly, we report evidence of a phospho-relay from autophosphorylated IKK2 to IκBα in the presence of ADP. These observations suggest an unusual evolution of IKK2, in which autophosphorylation of tyrosine(s) in the activation loop, and the conserved ATP-contacting K44 residue provide its signal-responsive substrate specificity and ensure fidelity during NF-κB activation.

Introduction:

Protein kinases confer novel identity and, often, novel functionality to their substrates by adding phosphate moieties to specific sites, thus playing key regulatory roles in a diverse array of signaling systems. One such example is the action of Inhibitor of κB Kinase-complex (IKK-complex), which is composed of two catalytic subunits, IKK1 (also known as IKKα) and IKK2 (or IKKβ), and an essential regulatory scaffolding protein, NEMO (IKKγ). IKK-complex precisely triggers induction of NF-κB family transcription factors in metazoans in response to inflammatory or pathogenic signals (Hoffmann and Baltimore, 2006)(DiDonato et al., 1997; Rothwarf et al., 1998; Zandi et al., 1997). In resting cells, activity of IKK2 is maintained at a low basal level (Ghosh and Karin, 2002; Hacker and Karin,

2006; Hinz and Scheidereit, 2014; Liu et al., 2012). In response to inflammatory or pathogenic signaling cues, the IKK2 subunit becomes activated via phosphorylation at two serine residues within its activation loop and subsequently phosphorylates two critical serine residues (S32 and S36) near the N-terminus of IκBα (Inhibitor of NF-κB α), marking the inhibitor protein for ubiquitin-dependent 26 *S* proteasome-mediated degradation (Figure 1A). Signal-responsive phosphorylation of IκBα refers to phosphorylation of its S32 and S36 residues by the IKK-activity. Degradation of IκBα liberates NF-κB, which then translocates to the nucleus to execute its gene expression program (Hayden and Ghosh, 2008; Hinz and Scheidereit, 2014; Karin and Ben-Neriah, 2000; Scheidereit, 2006). Mutation of IκBα residues S32 and S36 to phospho-ablative alanine converts it into a super-repressor of NF-κB that is incapable of being degraded in response to NF-κB signaling (Brown et al., 1995; Lin et al., 1995), highlighting the need for exquisite specificity of IKK2 in phosphorylating these two serines (DiDonato et al., 1997). The IKK2 subunit fails to phosphorylate IκBα when S32 and S36 are mutated even to threonine, another phosphorylatable residue. Despite its critical role in the regulation of NF-κB via high fidelity phosphorylation specificity toward IκBα, IKK2 behaves with functional pleiotropy toward other substrates and in other contexts (Antonia et al., 2021; Schröfelbauer et al., 2012; Schrofelbauer and Hoffmann, 2011).

IKK2 is a multidomain protein consisting of a kinase domain (KD) in association with a ubiquitin-like domain (ULD) followed in sequence by a scaffold dimerization domain (SDD) and a C-terminal region that contains the NEMO-binding domain (NBD) (Figure 1B). As mentioned previously, the hitherto enigmatic activation of IKK2 from its inactive state is manifested in the phosphorylation status of two serine residues, S177 and S181 (S176 and S180 for IKK1), located within in the activation loop (AL) of the KD (Huse and Kuriyan, 2002; Liu et al., 2013; Polley et al., 2013; Xu et al., 2011). Phospho-mimetic substitution of these two serines to glutamates (S177E, S181E; henceforth EE) renders IKK2 constitutively active. It has been demonstrated that the upstream kinase TAK1 primes IKK2 through

phosphorylation at S177, leading to its autophosphorylation at S181 and full activation in cells (Zhang et al., 2014). Alternatively, it has also been shown that increased oligomerization upon association with NEMO and linear or Lys63-linked poly-ubiquitin chains, or due to a high concentration of IKK2, enables *trans* autophosphorylation of IKK2 at S177 and S181 (Chen, 2012; Du et al., 2022; Ea et al., 2006; Polley et al., 2013). NEMO appears not only to aid in activation of the IKK-complex, but also to direct IKK activity towards IκBα bound to NF-κB (NF-κB:IκBα complex) (Schröfelbauer et al., 2012). The SDD of IKK2 and the C-terminal segment (residues 410-756, collectively) are also required for specific phosphorylation of IκBα at S32 and S36. A shortened version of IKK2 with deletion of these regions failed to retain the above-mentioned exquisite specificity of IKK2 but phosphorylated IκBα at serine and threonine residues within its C-terminal PEST (residues 281-302) region (Shaul et al., 2008). Interestingly, this C-terminal PEST region of IκBα, which is rich in proline, glutamic acid, serine, and threonine residues, is phosphorylated *in vivo* by other kinases that are not capable of phosphorylating IκBα at S32 and S36 (Barroga et al., 1995; Tergaonkar et al., 2003). Despite its central role in the regulation of transcription factor NF-κB, the connection or interdependence of IκBα phosphorylation at the PEST region and the signal responsive S32/S36 sites remains elusive.

In this study, we employed structure-based biochemical and cell-based experimental approaches to explore the basis of IKK2 specificity towards S32/S36 of IκBα that is required for rapid induction of NF-κB transcriptional activity in response to canonical signaling. Biochemical analysis of catalytically competent IKK2 revealed that it is capable of autophosphorylation at tyrosine residues in addition to autophosphorylation of its own serines or phosphorylation of serines in its substrate IκBα. Therefore, IKK2 is a dual-specificity protein kinase. IKK2 tyrosine autophosphorylation depends upon prior phosphorylation of activation loop S177/S181 and plays a significant role in phosphorylation of signal responsive S32/S36 of IκBα. The phosphorylation of IκBα at S32 was severely compromised upon substitution of Y169 of IKK2 to a phospho-ablative phenylalanine.

Additionally, signal-responsive phosphorylation of IκBα upon TNF-α treatment in MEF cells reconstituted with IKK2-Y169F was severely diminished in comparison to wild type IKK2 (IKK2-WT). We also observed that an IKK2 bearing the K44M mutation resulted in a loss of S177 and S181 as well as tyrosine autophosphorylation activities and consequent loss of S32/S36 phosphorylation in IκBα, confirming a critical function of this lysine residue. Interestingly, phosphorylation of residues within the C-terminal PEST region of IκBα was retained in IKK2-K44M. Finally, we observed an intriguing activity of IKK2, when fully autophosphorylated at its serine and tyrosine residues, to phosphorylate IκBα in the absence of an exogenous supply of ATP, if ADP is present in the reaction. This result suggests the possibility of a unique, and likely transient, autophosphorylated form of IKK2 that can serve to relay phosphoryl group(s) specifically to S32/S36 of IκBα. Such a mechanism contrasts with the conventional transfer of γ-phosphate groups directly from ATP to the substrate observed in eukaryotic protein kinases.

Results:

IKK2 undergoes autophosphorylation at uncharacterized sites:

Signal-induced phosphorylation of activation loop residues Ser177 and Ser181 is the hallmark signature of IKK2 catalytic activity (Figure 1B). In contrast, hyperphosphorylation of other serine residues located within the flexible C-terminal region of IKK2, spanning amino acids 701 to 756 (Figure 1B), has been reported to down-regulate IKK2 activity in cells (Delhase et al., 1999). Ectopically overexpressed IKK2 has been observed to autophosphorylate the two serines of the activation loop in *trans* even in the absence of an activating physiological signal {Polley, 2013 #27}. We observed that purified recombinant full length IKK2 is autophosphorylated when incubated with ATP in the absence of NEMO in a time-dependent manner, and likely at multiple sites as indicated by the diffuse nature of the slower migrating phospho-IKK2 band (Figure 1C). The autophosphorylated IKK2 produced a sharper band in the presence of NEMO – possibly reflecting enhanced specificity of phosphorylation (Figure 1D, left panel) – although NEMO did not alter the efficiency of

phosphorylation for its *bona fide* substrate IκBα (Figure 1D, right panel). An *in vitro* kinase assay with a K44M mutant of IKK2 that lacks both its autophosphorylation and IκBα phosphorylation activities along with the native sequence IKK2 using γ-^{32}P-ATP confirmed that phosphorylation of IKK2 was self-catalyzed and not due to a spurious contaminating kinase (Figure 1 - figure supplement 1A). K44 is an ATP-contacting residue that is conserved across STYKs, including IKK2, and its mutation to methionine typically reduces or eliminates kinase activity. An *in vitro* kinase assay showing inhibition of specific phosphorylation of S32/36 on IκBα and IKK2-autophosphorylation performed in the presence of an IKK-specific ATP-competitive inhibitor, Calbiochem Inhibitor VII, further validates that phosphorylation of IKK2 is due to its own activity (Figure 1E, Figure 1 - figure supplement 1B). In these experiments, the reaction mixtures of kinase and kinase:substrate were incubated with the inhibitor for 30 minutes prior to addition of the phosphate donor, γ-^{32}P-ATP or cold ATP. Purity of recombinant IKK2 and IKK2 K44M proteins is shown in Figure 1 - figure supplement 1C, and an LC-MS/MS analysis of the IKK2 K44M is shown in Figure 1 - figure supplement 1D.

Next, we performed kinase assays with variants of IKK2 protein with activation loop S177 and S181 mutated to phospho-mimetic glutamate resulting in the constitutively active IKK2-EE mutant form (Zandi et al., 1998) and with the C-terminal serine-rich region truncated to various extents. The shortest construct, Δ664EE, which lacked the entire flexible C-terminal region (670-756), was subjected to limited proteolysis using trypsin to further eliminate flexible N- and C-terminal residues and subsequently purified for *in vitro* kinase assays. These deletion IKK2-EE constructs displayed both autophosphorylation and substrate IκBα phosphorylation activities (Figure 1F). The observed autophosphorylation of IKK2 lacking serines of the activation loop and the C-terminal segment suggested the existence of hitherto uncharacterized sites of autophosphorylation in IKK2.

Autophosphorylation of IKK2 reveals its dual specificity:

We were intrigued as to whether the observed autophosphorylation activity of IKK2 might involve other residues in addition to the previously characterized serines, i.e., the possibility of IKK2 being a dual specificity kinase. Indeed, we observed by western blot with anti-phosphotyrosine antibodies the unexpected *de novo* autophosphorylation of IKK2 at tyrosine residues (Figure 2A, middle panel) in addition to the previously reported autophosphorylation of activation loop serines (Figure 2A, upper panel) when full length native sequence IKK2 was incubated with Mg^{2+}-ATP for various amounts of time. Increased autophosphorylation of activation loop S177 and S181 over time reflects nonhomogeneous and incomplete phosphorylation of activation loop S177 and S181 in the IKK2 obtained from recombinant baculovirus-infected Sf9 insect cells. To address the possibility of non-specificity by the pan-phosphotyrosine antibody (used in Figure 2A), we further performed the experiment with an alternate anti-phosphotyrosine specific antibody that confirmed detection of *de novo* tyrosine phosphorylation was independent of the source of the antibody used (Figure 2B). ATP-dependent tyrosine autophosphorylation was not observed in the presence of an IKK-specific inhibitor, Inhibitor VII (Figure 2C), and with the kinase inactivating IKK2 K44M mutant (Figure 2D). Additionally, autophosphorylation assays performed in the presence of urea revealed tyrosine autophosphorylation to be undetectable at urea concentrations greater than 1M (Figure 2 – figure supplement 1A). More sensitive assays using γ-^{32}P-ATP recapitulated elimination of pan-autophosphorylation and IκBα substrate phosphorylation of IKK2 above 1M urea (Figure 2 – figure supplement 1B). These results demonstrate the dual specificity of recombinant IKK2 in phosphorylating serine residues on itself and on substrates, as well as tyrosine residues on itself. The fact that activities of IKK2 towards S32 and S36 of IκBα and its own tyrosine residue(s) were affected similarly by both general (AMPPNP and Staurosporine) and IKK-specific (MLN-120B, TPCA, Inhibitor VII) (Figure 2 – figure supplement 1C) kinase inhibitors, indicates that both activities occur in the same active site. Using various truncated versions of IKK2, we further observed that the C-terminal NBD of IKK2 is not required for its autocatalytic dual specificity, and in

phosphorylating IκBα at S32 and S36 (Figure 2E) *in vitro*. Semi-quantitative assessment of phospho-Ser and phospho-Tyr residues on a constitutively active NBD-deficient IKK2 (IKK2Δ664EE) was performed by western blot with monoclonal anti-phosphoserine and anti-phosphotyrosine antibodies, which revealed *de novo* autophosphorylation at tyrosine residues but not at serines (Figure 2F). The phospho-ablative S177A/S181A (AA; non-phosphorylatable activation loop) mutant of IKK2, that is incapable of phosphorylating S32 and S36 of IκBα (Figure 2 – figure supplement 1D), also lacked tyrosine autophosphorylation activity (Figure 2G) in an *in vitro* kinase assay suggesting phosphorylation of activation loop S177/S181 to be critical for dual specificity of IKK2.

Dual-specific autophosphorylation is critical for function of IKK2:

Previous reports suggested that phosphorylation of IKK2 on Y169, Y188, and/or Y199 is critical for its function (Darwech et al., 2010; Meyer et al., 2013). We performed mass spectrometric analyses on *in vitro* autophosphorylated IKK2 and identified Y169 to be the prominent tyrosine autophosphorylation site (Figure 3 – figure supplement 1A). To explore the possible relevance of phosphorylation at tyrosine residues within the activation loop to kinase catalytic activity, we analyzed the experimentally determined x-ray crystal structures of IKK2 monomers within reported models of human IKK2 dimers (PDB ID: 4KIK, 4E3C) (Liu et al., 2013; Polley et al., 2013). In the active state conformers, the position and conformation of Tyr169 appears to be well positioned for accepting a phosphate from ATP intramolecularly (Figure 3 – figure supplement 1B). A superposition of IKK2 with a pseudo-substrate-bound PKA shows that the hydroxyl of Tyr169 in IKK2 projects toward the γ-phosphate of ATP similarly to the serine hydroxyl on the PKA inhibitor pseudo-substrate (Knighton et al., 1991; Nolen et al., 2004) (Figure 3 – figure supplement 1B and 1C). Interestingly, the position occupied by Y169 in IKK2 primary sequence corresponds to the classic DFG+1 (DLG in cases of IKK2 and IKK1) (Figure 3A & B). The DFG+1 position has been reported to be critical in defining the substrate specificity of a kinase (Chen et al., 2014).

We primarily focused our attention to the previously described K44M mutant and the newly generated Y169F mutant of IKK2, since these residues are located within the vicinity of the enzyme active site. We observed that the IKK2 K44M mutant fails to undergo autophosphorylation of tyrosine (Figure 2D) and the activation loop serines (Figure 3 – figure supplement 1D). Surprisingly, IKK2 K44M displayed a very weak (compared to that of WT IKK2) autophosphorylation activity but a more robust phosphorylation of full length IκBα, albeit to a much lesser degree than native sequence IKK2, in a radioactive *in vitro* kinase assay (Figure 3C). Interestingly, we observed a lack of phosphorylation of IκBα at S32 and S36 by IKK2 K44M (Figure 3D). This suggests that IKK2 K44M phosphorylates IκBα at residues within its C-terminal PEST, consistent with the observed phosphorylation of IκBα (Figure 3C & D). Moreover, IKK2 K44M phosphorylated super-repressor IκBα S32A/S36A more efficiently than native sequence IκBα, in sharp contrast to IKK2 of native sequence (Figure 3 – figure supplement 1E). This suggests that IKK2 K44M retains significant kinase activity towards IκBα, though it is incapable of specific IκBα phosphorylation at S32,S36. LC-MS/MS analysis with 20 μg of Sf9-derived IKK2 K44M protein used in our studies did not indicate the obvious presence of any contaminating kinase. It is noteworthy that an equivalent K to M mutant of Erk2 retained ~5 % of its catalytic activity (Robbins et al., 1993).

Next, we assessed the activity of a tyrosine-phosphoablative Y169F mutant of IKK2 in an *in vitro* kinase assay and observed a severe reduction in both autophosphorylation and IκBα phosphorylation activities (Figure 3E). We measured its phosphorylation activity towards native sequence IκBα as well as IκBα with either S32 or S36 residues independently substituted to either phosphoablative alanine or phosphomimetic glutamic acid. IKK2 Y169F displayed drastically reduced levels of kinase activity towards S36A/E mutants of IκBα while the S32A/E mutants were minimally affected when compared against the native IκBα substrate (Figure 3F). The reduction in phosphorylation of S36A/E by IKK2 was less pronounced than that by IKK2 Y169F (Figure 3 – figure supplement 1F). These

observations suggest that the tyrosine residue at position 169 (and possibly its phosphorylation) might contribute towards signal-responsive phosphorylation of IκBα.

We also measured signal-induced activation of IKK2 upon TNF-α treatment in *ikk2*$^{-/-}$ mouse embryonic fibroblast (MEF) cells reconstituted with native sequence IKK2 and IKK2 Y169F. Catalytic activity is significantly reduced in IKK2 Y169F (Figure 3G**)**. Nonetheless, phosphorylation of activation loop serines was only marginally defective for IKK2 Y169F as judged by anti-phosphoserine-177 western blot (Figure 3 – figure supplement 1G) hinting at the necessity, but not sufficiency, of activation loop phosphorylation for IKK2 to become fully active. Together, these results imply a possible interdependence of phosphorylation at Y169 of IKK2 and S32 of IκBα.

Structural analyses of IKK2 autophosphorylation:

We next analyzed three states of IKK2: unphosphorylated (UnP-IKK2), phosphorylated at S177 and S181 (p-IKK2), and phosphorylated at Y169, S177, and S181 (P-IKK2) using computational approaches of molecular dynamic (MD) simulations of 200 ns scale and flexible molecular docking (see methods)[43–50]. Phosphorylation at S177 and S181 increased folding stability of the kinase, which was further stabilized by phosphorylation at Y169 as evidenced by a gradual decrease in the total energy of the system (Figure 4A). Results of differential scanning calorimetry (DSC) in the presence of ADP vs. ATP also indicated a change of Tm from ~40°C to ~50°C i.e., reflecting a striking enhancement in stability upon autophosphorylation of IKK2 (Figure 4 – figure supplement 1A). These results correlate with observations of increased solubility of IKK2 upon autophosphorylation; a property found to be essential for its successful crystallization (Polley et al., 2013).

Counterintuitively, we observed the highest RMSD for P-IKK2, followed by p-IKK2, and then UnP-IKK2 (Figure 4B). This result might be indicative of an increased internal motion despite phosphorylation-induced stabilization of IKK2 because of phosphorylation. The changes in total energy and RMSD values were consistent throughout the course of simulation even though the magnitude was small. We observed distinct structural alteration

within the KD upon phosphorylation at S177 and S181 or S177,S181, and Y169 (Figure 4C, models shown separately in Figure 4 – figure supplement 1B). Analyses of the trajectory of RMSF values for the three states revealed different regions of the kinase domain with different RMSF values in different phosphorylated states (Figure 4 – figure supplement 1C). We observed that, while the glycine-rich loop and the αC-helix in p-IKK2 were positioned in a manner reminiscent of an active kinase, those in UnP and P-IKK2 were oriented differently (Figure 4C). In fact, helix αC was found to be distorted in P-IKK2 in a manner that would make it unlikely to support canonical phosphotransfer from ATP. The activation loop in these three states adopted conformations distinct from each other. The activation loop in the UnP model was splayed out and moved closer to the tip of the C-lobe, whereas the activation loop in p-IKK2 and P-IKK2 moved inwards and adopted more compact conformations closer to the N-lobe (Figure 4C). The formation of the proper R- and C-spines in p-IKK2 confirmed its active conformation (Figure 4D). The p-IKK2 KD exhibited additional features consistent with an active kinase: a salt bridge between K44 and E61 (K72 and E91 in PKA, respectively), and the 'DFG in' conformation (though the sequence is DLG in IKK2). In addition, a dynamic cross-correlation matrix (DCCM) or contact map of each structure suggests that specific phosphorylation events render distinct allosteric changes to the kinase, even at locations distant from the phosphorylation sites (Figure 4 – figure supplement 1D).

Next, we docked ATP onto IKK2 structures in all three states using LeDock and GOLD followed by rescoring with AutoDock Vina using the 0 ns (starting, S) and 200 ns (ending, E) structures of our MD simulation studies (see methods). The results indicated that ATP binding to P-IKK2 is relatively unfavorable (docking score in positive range) in both starting and ending structural models (Figure 4 – figure supplement 1E), whereas ATP binding to UnP-IKK2 and p-IKK2 is favorable. ADP binding is however favorable for all phosphorylated or unphosphorylated IKK2 structural models except for the starting conformation of P-IKK2 (Figure 4 – figure supplement 1E). We also extracted 50

intermediate structures from a 10 ns MD simulation run and calculated their binding free energies (ΔG) using the MM-PBSA (Molecular Mechanics Poisson-Boltzmann Surface Area) method. We again observed that ATP-binding for the P-IKK2 population is highly unfavourable in contrast to their high relative preference for ADP, whereas p-IKK2 displayed comparable preference for both ATP and ADP (Figure 4 – figure supplement 1F). In the ATP-docked structures, the ATP phosphate groups exhibited a pose (ΔG = -10.64 kcal/mol) very similar to that observed in the PKA structure (PDB ID: 1ATP) (Figure 4 – figure supplement 1G), and the terminal phosphate was in close proximity to the Y169-OH, consistent with the likelihood of autophosphorylation at Y169 (Figure 4E). Further analyses of the ATP-bound p-IKK2 structure confirmed that the presence of ATP enhanced formation of the R- and C-spines, as observed in active forms of kinases (Figure 4F). Superposition of the ATP from the p-IKK2 on P-IKK2 indicated that narrowing of canonical the ATP-binding pocket in P-IKK2 may lead to rejection of ATP from the canonical binding pocket, triggered by severe clashes between the glycine-rich loop and ATP (Figure 4G). However, this does not exclude the possibility that P-IKK2 might interact with ATP through alternative binding modes. Furthermore, the R-spine in P-IKK2 exhibited a discontinuity (Figure 4H), with M65 (L95 in PKA) located away from the other three conserved spine residues, and from the glycine-rich loop.

Binding of ATP to p-IKK2 could lead to autophosphorylation at Y169, thus generating P-IKK2 bound to ADP. The superposition of ADP (from the docked complex of p-IKK2 and ADP, ΔG = -9.88 kCal/mol, Figure 4I) onto the P-IKK2 structure confirmed that while P-IKK2 is unable to accommodate ATP in a manner similar to that observed in experimentally determined kinase structures, it could accommodate ADP into the ATP-binding cleft comfortably (Figure 4J). The affinities of ATP and ADP for p-IKK2 appears comparable as indicated by their respective binding energy/docking score values, like in other kinases (Becher et al, 2012 PMID: 23215245). Thus, the cellular concentrations of ATP vs ADP could play an important role in kinase activity. We speculate that ADP-bound P-IKK2,

containing various and perhaps transiently phosphorylated groups within the activation loop and in close proximity to the active site, could act as an intermediate to relay phosphates back to ATP or to substrates.

These observations of IKK2 structural propensities hint at the possibility of residues within the flexible activation loop undergoing context-sensitive autophosphorylation and possibly rendering IKK2 with novel phospho-transfer activities distinct from the conventional direct transfer of γ-phosphate from ATP to substrate.

Freshly autophosphorylated IKK2 phosphorylates IκBα even in absence of ATP:

We observed phosphorylation of tyrosine residue(s) only upon ATP-treatment of purified IKK2 proteins, hinting at the likelihood of efficient cellular phosphotyrosine phosphatases (Eckhart et al., 1979). Surprisingly, crystal structures of Sf9-derived human IKK2 did not indicate phosphates on tyrosine residues even though recombinant IKK2 was treated with Mg^{2+}-ATP as part of the purification (PDB ID: 4E3C) (Polley et al., 2013). It is unclear if the month-long period of crystallization at 18-20°C contributed to loss of the generally very stable phosphotyrosine residues. This raises the intriguing possibility that phosphotyrosine residue(s) in IKK2 might somehow serve as a transient sink of phosphate for its eventual transfer to ADP or serines in the IκBα substrate. To investigate this hypothesis, we first incubated purified IKK2 with limiting amounts of radiolabeled γ-^{32}P-ATP for autophosphorylation and subsequently removed unreacted ATP via two passes through desalting spin columns (40 kDa MWCO). The nucleotide-free autophosphorylated IKK2 (P-IKK2) was then incubated with substrate IκBα either in the absence or with the fresh addition of unlabeled ATP/ADP. Resolution of the reaction mixture on an SDS-PAGE and subsequent autoradiography indicated transfer of radiolabeled phosphate to IκBα (Figure 5A), which was significantly enhanced in the presence of cold ADP (Figure 5B). Addition of excess cold ATP did not reduce the extent of IκBα phosphorylation, strongly suggesting the transfer of ^{32}P-phosphate from ^{32}P-IKK2 to IκBα (Figure 5B) and consistent with an IKK2-

mediated phosphate relay mechanism. It is unclear if the transfer of phosphate from the phospho-IKK2 intermediate to IκBα occurs with or without direct involvement of ADP.

To further investigate the possibility of transfer of phosphate from the kinase (and not from ATP) to the substrate, we produced autophosphorylated IKK2 obtained by treatment of recombinant full length IKK2 with excess cold ATP and purified using size-exclusion chromatography on a Superdex200 column to remove any traces of unreacted ATP (Figure 5C). P-IKK2 eluted at SEC fractions corresponding to MW between 670 and 158 kDa, much earlier than free ATP (Figure 5D). This P-IKK2 was incubated with IκBα substrate either in the presence or absence of ADP for varying time periods. A similar reaction was set up in the presence of ATP instead of ADP as a positive control. We observed, by western blot with sequence-specific anti-phosphoserine antibody, efficient phosphorylation of IκBα S32 and S36 residues in the presence of ADP (10 and 50 μM) but not in its absence. As anticipated, a robust phosphorylation of IκBα was observed in the presence of 50 μM ATP (Figure 5E). The very low-level detection of IκBα phosphorylation by radioactive assay in the absence of ADP and complete lack of signal in the cold immunoblotting assay (compare lanes marked with vertical arrows in Figures 5B and 5E) may indicate higher sensitivity of the radioactive assay. We quantified the intensities of each band in Figure 5E, and the ratios of the normalized average intensities of the tyrosine phosphorylated IKK2 and S32/36-phosphorylated IκBα with their respective full-length protein controls were plotted as shown in Figure 5 – figure supplement 1A. Next, we followed the same experimental scheme as shown in Figure 5C and assessed IκBα phosphorylation by relay mechanism at a finer time interval. Phosphorylation of S32/S36 of IκBα increased with time as shown in Figure 5 – figure supplement 1B. The requirement for ADP in the observed phosphotransfer prompted us to consider if our ADP was contaminated with trace amounts of ATP. ESI-MS analysis of our 50 μM ADP solution did not detect any peak corresponding to ATP (Figure 5 – figure supplement 1C). Dependence of IκBα phosphorylation on ADP raises the possibility of infinitesimal reversibility generating ATP from ADP in the active site of the kinase. We could

not detect the generation/presence of ATP in a setting similar to that described in Figure 5A & B by TLC-based analysis (Figure 5 – figure supplement 1D).

Phosphotransfer from P-IKK2 is critical to fidelity and specificity of IκBα phosphorylation:

We next tested whether the observed phosphotransfer to IκBα is restricted only to the S32 and S36 residues required for NF-κB activation or also directed toward serine/threonine residues within C-terminal PEST domain of IκBα. Kinase assays performed with P-IKK2 and IκBα of native sequence or harboring S32A and S36A mutations (AA) in the presence of γ-^{32}P-ATP revealed a lack of phosphorylation of IκBα AA, though that protein retains the serines and threonines of the C-terminal PEST region (Figure 6A). Furthermore, a similar assay with IKK2-Y169F showed its inability to transfer phosphate to IκBα (Figure 6 – figure supplement 1). Taken together, this hints at transfer of phosphate exclusively to S32 and S36 of IκBα from Y169. We also observed no inhibitory effect on the phosphotransfer by AMPPNP, an unhydrolyzable analogue of ATP, irrespective of the presence of ADP. This suggests that diverse adenine nucleotides prompt phosphotransfer by the kinase (Figure 6A). It is noteworthy that a recent study reported that IKK2 phosphorylates IκBα sequentially at S32 followed by S36 following a single binding event and that phosphorylation of S32 increases the phosphorylation rate of S36 (Stephenson et al., 2022).

Taken together with our results, we propose that catalytically active IKK2, that is by definition phosphorylated at S177 and S181, can undergo autophosphorylation on tyrosine residues within its activation loop. Furthermore, the tyrosine autophosphorylated IKK2 could serve as a phosphoenzyme intermediate to transfer its phosphate group to S32 of IκBα, thereby enhancing the rate of phosphorylation at S36, possibly using ATP for the second site phosphorylation at S36 (Figure 6B).

Discussion:

The phosphorylation of cognate substrates by protein kinases is regulated in a variety of ways (Cullati et al., 2022; Sang et al., 2022). IKK2, a kinase central to

inflammation, phosphorylates serine residues of its primary substrate IκBα using γ-phosphate of ATP. In this study, we report several intriguing structural and biochemical properties of IKK2 that contribute to its substrate phosphorylation specificity and efficiency: 1) dual-specificity of IKK2 that entails autophosphorylation of its own tyrosine residues, in addition to known autophosphorylation of activation loop serines; 2) loss of specificity, but retention of diminished catalytic activity, upon disruption of a universally conserved salt bridge mediated by K44 in IKK2; and 3) relay of phosphate to substrate IκBα from autophosphorylated IKK2 (P-IKK2).

Dual specificity of IKK2: Our present analyses of IKK2 revealed a surprising property wherein IKK2 phosphorylated at activation loop serines S177/S181 could be further autophosphorylated by ATP at multiple sites, including at least one of its tyrosine residues, yielding a hyper-phosphorylated form (P-IKK2) (Figure 6B). This defines IKK2 as an autocatalytic dual-specificity kinase rather than simply a prototypical Ser/Thr kinase. Several members of the Ser/Thr kinase family have been reported to undergo tyrosine phosphorylation and it appears that many of these kinases employ diverse strategies for phosphorylation (Bhattacharyya et al., 2006; Ge et al., 2002; Lochhead, 2009; Lochhead et al., 2006, 2005; Sugiyama et al., 2019; Tigno-Aranjuez et al., 2010). Tyrosine residues within the activation loop of IKK2 are also reported to undergo signal-induced phosphorylation in cells, and this is proposed to be mediated by a tyrosine kinase (Meyer et al., 2013; Otero et al., 2008; Rieke et al., 2011). However, dual specificity is notably manifested by DYRK and GSK3β, even though function of tyrosine phosphorylation in DYRK/GSK3β does not appear to be related to that of IKK2.

The phosphorelay mechanism: The Ser/Thr/Tyr family of eukaryotic protein kinases transfer γ-phosphate of ATP directly to substrates, usually at S, T, and Y residues (Cohen, 2002; Fischer and Krebs, 1955; Hunter, 1991; Krebs and Fischer, 1955; Nolen et al., 2004). In contrast, histidine kinases found in prokaryotes and in some simple eukaryotes employ a mechanism in which the γ-phosphate of ATP is transferred first to an aspartate residue on a

response regulator (RR) substrate through an internal phosphohistidine intermediate (Borkovich and Simon, 1990; Gao and Stock, 2009; Hunter, 2022; Kalagiri and Hunter, 2021; Laub et al., 2007; Robbins et al., 1993). Surprisingly, the hyper-phosphorylated P-IKK2 appears to display an ability to transfer phosphate(s) to substrate IκBα in the presence of ADP without requiring an exogenous supply of fresh ATP – hinting at the possibility of IKK2 acting as a phosphate sink capable of relaying phosphate from the phophoenzyme intermediate to the substrate (Figure 5B & 5E). Since this phosphotransfer to S32 and S36 of IκBα is observed with autophosphorylated, constitutively active IKK2 EE, the transferred phosphates are unlikely to derive from phosphorylated S177 or S181. Phosphorylated Y169, on the other hand, could be a suitable candidate to act as an intermediate and a source of transferable phosphate due to its conducive location at the DFG+1 (DLG in IKK2) position. Y169 seems particularly fit for this role as it is the only active site-proximal residue prominently autophosphorylated within the activation loop of IKK2 (Figure S3A). Tyrosine at this position is unique only to IKK1 and IKK2 and the plant kinase SNRK1, and is absent even in close mammalian orthologs such as IKKε and TBK1 (Larabi et al., 2013; Tu et al., 2013). Interestingly, a study has implicated the role of DFG+1 residue in differentiating kinase specificity towards Ser versus Thr residues (Chen et al., 2014). These observations hint at the possibility of Y169 being involved in phosphorylation selectivity of IκBα substrate. We observed a role for Y169 in phosphorylating S32 of IκBα using both *in vitro* and *ex vivo* experiments (Figure 3F & G); however, our data does not confirm if Y169 phosphorylation is the sole contributor to specific signal-responsive phosphorylation of IκBα. It is noteworthy that a S32I mutant of IκBα containing the phosphoablative mutation at S32 is associated with ectodermal dysplasia and T-cell immunodeficiency (Courtois et al., 2003; Mooster et al., 2015). Autophosphorylation in the kinase domain has been observed to regulate function in other kinases as well, e.g., autophosphorylation at T220 greatly influenced both the activity and substrate specificity of CK1 (Cullati et al., 2022). So far, IKK2 appears to be the only other metazoan protein kinase that derives its substrate specificity through the formation of a

phosphoenzyme intermediate apart from MHCK of *Dictyostelium discoideum* (an atypical eukaryotic protein kinase) (Ye et al., 2010). The transfer of phosphate from Tyr169 to Ser32 of IκBα represents an intriguing and unprecedented mechanism among metazoan protein kinases. We propose a possible explanation for the process: the hydroxyl group of Tyr169 is optimally positioned to readily accept the γ-phosphate from ATP at the expense of minimal energy in presence or absence of the substrate IκBα. This relay of phosphate – from ATP to Tyr169 to Ser32 – might offer a more energetically favorable pathway than a direct transfer of phosphate from ATP to the substrate. Another intriguing feature of phosphorelay in IKK2 is its dependence on ADP (Figure 5B & E), which the generic kinase inhibitor AMPPNP (unhydrolyzable ATP analogue) failed to inhibit (Figure 6A). Taken together, we surmise that ADP or AMPPNP might act as an ATP surrogate in helping IKK2 adopt a conformational state commensurate with selective phosphorylation of S32 and S36 in IκBα. A similar phenomenon is reported for IRE1, where ADP was found to be a potent stimulator of its ribonuclease activity and AMPPNP was also reported as a somewhat effective potentiator (Lee et al., 2008; Sidrauski and Walter, 1997). We speculate that Ser32 cannot be efficiently phosphorylated by p-IKK2:ATP due to a deliberate chemical mismatch of the hydroxyl group of Ser32 within the active site. However, it aligns well with the P-IKK2:ADP intermediate. Indirect supporting evidence, as described above, underscores the existence of a unique phosphotransfer mechanism; however, detailed structural, biochemical and MD simulations studies are necessary to validate this model.

Signaling specificity and digital activation: The amplitude, duration, and kinetics of IKK activity correlate with the strength of input signal, level of IκBα degradation, and NF-κB activation (Behar and Hoffmann, 2013; Cheong et al., 2006). This digital (all-or-none) activation profile of NF-κB appears to be due to rapid activation and inactivation of IKK2. The primary target of IKK2 is IκBα which underlies the rapid activation of NF-κB, although multiple other substrates are targeted *in vivo*. This digital activation profile may be intrinsically linked to the phosphorelay process. The selection of specific IκBα residues for

phosphorylation is unclear, although NEMO is reported to have a direct role (Schröfelbauer et al., 2012). We observe that P-IKK2 transfers phosphate(s) efficiently and specifically to S32 and S36 of IκBα, but not to other phosphorylatable sites, such as the serine and threonine residues within the IκBα C-terminal PEST region (Figure 5B, 5E, and 6A). We surmise that the transiency of various phosphorylated residues in P-IKK2 could underlie the activation-inactivation event during signal response. In this context, it will be worth investigating if functional regulation of IKK2 involves properties analogous to that of the two-component histidine kinase-effector systems (Bhate et al., 2015; Lamarche et al., 2008; Laub and Goulian, 2007). It is noteworthy that phosphate transfer directly from phosphohistidine is energetically far more favorable than from phosphotyrosine, except in enzymatic processes. The phosphotransfer from P-IKK2 to IκBα investigated and reported herein reflects a single turnover event in the absence of the phosphate donor, ATP (Figure 5B). Not every phosphorylated residue over the long span of the P-IKK2 is expected to have the ability to transfer its phosphate to IκBα and additionally, the P-IKK2 likely represents a pool with non-homogenous distribution of phosphorylated residues. This could be a reason for observance of the substoichometric phospho-relay.

The K44 conserved salt bridge is a determinant of specificity but not activity. We also observe a critical role of K44 in autophosphorylation of IKK2 and specific phosphorylation of S32 and S36 in IκBα. Interestingly, the IKK2 K44M mutant retained its non-specific kinase activity toward the C-terminal PEST region of IκBα. Along these lines, an engineered monomeric version of IKK2 (lacking its NBD and major portions of its SDD) was observed to retain specificity for the N-terminal serines of IκBα (Hauenstein et al., 2014), whereas a smaller version of IKK2 with only the KD and ULD lacked S32 and S36 specificity but retained the ability to phosphorylate IκBα within its C-terminal PEST region (Shaul et al., 2008). It is possible that a particular structural state of IKK2 or its interaction with a partner protein could direct IKK2 to phosphorylate specific sites within different substrates.

Conclusion: It is intriguing how the activation of NF-κB, through unique phosphorylation events catalyzed by IKK2, appears to be regulated by a complex and multi-layered fail-safe mechanism. In absence of upstream signals, the IKK-complex is unable to phosphorylate Ser 32/36 of IκBα efficiently thereby keeping a check on the aberrant and untimely activation of NF-κB. Upon encountering proinflammatory cues, cells need to activate NF-κB immediately, efficiently and specifically, i.e., IKK needs to be activated and phosphorylate Ser 32/36 of IκBα. NEMO warrants IKK-activation and ensures that the IKK-complex specifically chooses IκBα from a large pool of substrates of IKK2. IKK2 is designed in such a manner that it phosphorylates itself at an activation loop tyrosine when activated, such that phosphate group(s) can be relayed directly to Ser32/36 of IκBα with great fidelity, thus leaving little chance of a misconstrued signaling event thereby confirming NF-κB activation. Our discovery of an intriguing phosphotransfer reaction that helps accomplish the desired specificity could present the beginning of a new aspect in eukaryotic cell signaling by EPKs.

Methods summary:

Protein purification, autophosphorylation assay, immunoprecipitation-coupled kinase assay, phosphotransfer assay and other experiments are described in detail in the supplementary document.

Acknowledgement:

We thank Tony Hunter (Salk Institute) and Kaushik Biswas (Bose Institute) for commenting on the work, and members of Polley lab for their continuous support. This work was supported by an Intermediate Fellowship from the DBT Wellcome Trust India Alliance (IA/I/15/1/501852) & intramural funding from Bose Institute to SP, NIH grant to GG (AI163327), and American Cancer Society grant RSG-08-287-01-GMC and California Metabolic Research Foundation support to Biochemistry research at SDSU to TH. PB was supported by the graduate research fellowship from Bose Institute. SC acknowledges CSIR-IICB for infrastructure support. AC acknowledges ICMR for post-doctoral Research Associateship [BMI/11(55)2022].

Author contribution:

TB, GG, and SP designed experiments; PB, TB, GG, and SP performed biochemical experiments; PB prepared MS samples, PRT and SRC performed the MS analyses, AC and SC performed computational analyses; PB, TB, AC, TH, SC, GG, and SP analyzed data; PB, AC, SP prepared figures and images; SP wrote the manuscript; PB, TB, TH, and GG edited the manuscript.

Ethics declarations:

Competing interests: The authors declare no competing financial interests.

Data availability:

All computational data supporting the findings of this study are available in a repository on Zenodo (DOI: 10.5281/zenodo.15309725).

References:

Antonia RJ, Hagan RS, Baldwin AS. 2021. Expanding the View of IKK: New Substrates and New Biology. *Trends Cell Biol* **31**:166–178. doi:10.1016/j.tcb.2020.12.003

Barroga CF, Stevenson JK, Schwarz EM, Verma IM. 1995. Constitutive phosphorylation of I kappa B alpha by casein kinase II. *Proceedings of the National Academy of Sciences* **92**:7637–7641. doi:10.1073/pnas.92.17.7637

Behar M, Hoffmann A. 2013. Tunable Signal Processing through a Kinase Control Cycle: the IKK Signaling Node. *Biophys J* **105**:231–241. doi:10.1016/j.bpj.2013.05.013

Bhate MP, Molnar KS, Goulian M, DeGrado WF. 2015. Signal Transduction in Histidine Kinases: Insights from New Structures. *Structure* **23**:981–994. doi:10.1016/j.str.2015.04.002

Bhattacharyya RP, Reményi A, Good MC, Bashor CJ, Falick AM, Lim WA. 2006. The Ste5 scaffold allosterically modulates signaling output of the yeast mating pathway. *Science* **311**:822–826. doi:10.1126/science.1120941

Borkovich KA, Simon MI. 1990. The dynamics of protein phosphorylation in bacterial chemotaxis. *Cell* **63**:1339–1348. doi:10.1016/0092-8674(90)90429-i

Brown K, Gerstberger S, Carlson L, Franzoso G, Siebenlist U. 1995. Control of I kappa B-alpha proteolysis by site-specific, signal-induced phosphorylation. *Science* **267**:1485–1488. doi:10.1126/science.7878466

Chen C, Ha BH, Thevenin AF, Lou HJ, Zhang R, Yip KY, Peterson JR, Gerstein M, Kim PM, Filippakopoulos P, Knapp S, Boggon TJ, Turk BE. 2014. Identification of a major determinant for serine-threonine kinase phosphoacceptor specificity. *Mol Cell* **53**:140–7. doi:10.1016/j.molcel.2013.11.013

Chen ZJ. 2012. Ubiquitination in Signaling to and Activation of IKK. *Immunol Rev* **246**:95–106. doi:10.1111/j.1600-065X.2012.01108.x

Cheong R, Bergmann A, Werner SL, Regal J, Hoffmann A, Levchenko A. 2006. Transient IkappaB kinase activity mediates temporal NF-kappaB dynamics in response to a wide range of tumor necrosis factor-alpha doses. *J Biol Chem* **281**:2945–50. doi:10.1074/jbc.M510085200

Cohen P. 2002. The origins of protein phosphorylation. *Nat Cell Biol* **4**:E127–E130. doi:10.1038/ncb0502-e127

Courtois G, Smahi A, Reichenbach J, Döffinger R, Cancrini C, Bonnet M, Puel A, Chable-Bessia C, Yamaoka S, Feinberg J, Dupuis-Girod S, Bodemer C, Livadiotti S, Novelli F, Rossi P, Fischer A, Israël A, Munnich A, Le Deist F, Casanova J-L. 2003. A hypermorphic IkappaBalpha mutation is associated with autosomal dominant anhidrotic ectodermal dysplasia and T cell immunodeficiency. *J Clin Invest* **112**:1108–1115. doi:10.1172/JCI18714

Cullati SN, Chaikuad A, Chen J-S, Gebel J, Tesmer L, Zhubi R, Navarrete-Perea J, Guillen RX, Gygi SP, Hummer G, Dötsch V, Knapp S, Gould KL. 2022. Kinase domain autophosphorylation rewires the activity and substrate specificity of CK1 enzymes. *Mol Cell* **82**:2006-2020.e8. doi:10.1016/j.molcel.2022.03.005

Darwech I, Otero JE, Alhawagri MA, Abu-Amer Y. 2010. Tyrosine phosphorylation is required for IkappaB kinase-beta (IKKbeta) activation and function in osteoclastogenesis. *J Biol Chem* **285**:25522–25530. doi:10.1074/jbc.M110.121533

597 Delhase M, Hayakawa M, Chen Y, Karin M. 1999. Positive and Negative Regulation of IκB
598 Kinase Activity Through IKKβ Subunit Phosphorylation. *Science* **284**:309–313.
599 doi:10.1126/science.284.5412.309
600 DiDonato JA, Hayakawa M, Rothwarf DM, Zandi E, Karin M. 1997. A cytokine-responsive IκB
601 kinase that activates the transcription factor NF-κB. *Nature* **388**:548–554.
602 doi:10.1038/41493
603 Du M, Ea CK, Fang Y, Chen ZJ. 2022. Liquid phase separation of NEMO induced by
604 polyubiquitin chains activates NF-kappaB. *Mol Cell* **82**:2415-2426 e5.
605 doi:10.1016/j.molcel.2022.03.037
606 Ea CK, Deng L, Xia ZP, Pineda G, Chen ZJ. 2006. Activation of IKK by TNFalpha requires site-
607 specific ubiquitination of RIP1 and polyubiquitin binding by NEMO. *Mol Cell* **22**:245–
608 57. doi:10.1016/j.molcel.2006.03.026
609 Eckhart W, Hutchinson MA, Hunter T. 1979. An activity phosphorylating tyrosine in polyoma
610 T antigen immunoprecipitates. *Cell* **18**:925–933. doi:10.1016/0092-8674(79)90205-8
611 Fischer EH, Krebs EG. 1955. Conversion of phosphorylase b to phosphorylase a in muscle
612 extracts. *J Biol Chem* **216**:121–32.
613 Gao R, Stock AM. 2009. Biological Insights from Structures of Two-Component Proteins.
614 *Annu Rev Microbiol* **63**:133–154. doi:10.1146/annurev.micro.091208.073214
615 Ge B, Gram H, Di Padova F, Huang B, New L, Ulevitch RJ, Luo Y, Han J. 2002. MAPKK-
616 independent activation of p38alpha mediated by TAB1-dependent
617 autophosphorylation of p38alpha. *Science* **295**:1291–1294.
618 doi:10.1126/science.1067289
619 Ghosh S, Karin M. 2002. Missing pieces in the NF-kappaB puzzle. *Cell* **109 Suppl**:S81-96.
620 Hacker H, Karin M. 2006. Regulation and function of IKK and IKK-related kinases. *Sci STKE*
621 **2006**:re13. doi:10.1126/stke.3572006re13
622 Hauenstein AV, Rogers WE, Shaul JD, Huang DB, Ghosh G, Huxford T. 2014. Probing kinase
623 activation and substrate specificity with an engineered monomeric IKK2.
624 *Biochemistry* **53**:2064–73. doi:10.1021/bi401551r
625 Hayden MS, Ghosh S. 2008. Shared principles in NF-kappaB signaling. *Cell* **132**:344–62.
626 doi:10.1016/j.cell.2008.01.020
627 Hinz M, Scheidereit C. 2014. The IκB kinase complex in NF-κB regulation and beyond. *EMBO*
628 *Rep* **15**:46–61. doi:10.1002/embr.201337983
629 Hoffmann A, Baltimore D. 2006. Circuitry of nuclear factor kappaB signaling. *Immunol Rev*
630 **210**:171–86. doi:10.1111/j.0105-2896.2006.00375.x
631 Hunter T. 2022. A journey from phosphotyrosine to phosphohistidine and beyond. *Mol Cell*
632 **82**:2190–2200. doi:10.1016/j.molcel.2022.05.007
633 Hunter T. 1991. Protein kinase classification. *Methods Enzymol* **200**:3–37. doi:10.1016/0076-
634 6879(91)00125-g
635 Huse M, Kuriyan J. 2002. The conformational plasticity of protein kinases. *Cell* **109**:275–282.
636 doi:10.1016/s0092-8674(02)00741-9
637 Kalagiri R, Hunter T. 2021. The many ways that nature has exploited the unusual structural
638 and chemical properties of phosphohistidine for use in proteins. *Biochem J*
639 **478**:3575–3596. doi:10.1042/BCJ20210533
640 Karin M, Ben-Neriah Y. 2000. Phosphorylation meets ubiquitination: the control of NF-
641 [kappa]B activity. *Annu Rev Immunol* **18**:621–63.
642 doi:10.1146/annurev.immunol.18.1.621

643 Knighton DR, Zheng JH, Ten Eyck LF, Xuong NH, Taylor SS, Sowadski JM. 1991. Structure of a
644 peptide inhibitor bound to the catalytic subunit of cyclic adenosine monophosphate-
645 dependent protein kinase. *Science* **253**:414–420. doi:10.1126/science.1862343
646 Krebs EG, Fischer EH. 1955. Phosphorylase activity of skeletal muscle extracts. *J Biol Chem*
647 **216**:113–20.
648 Lamarche MG, Wanner BL, Crépin S, Harel J. 2008. The phosphate regulon and bacterial
649 virulence: a regulatory network connecting phosphate homeostasis and
650 pathogenesis. *FEMS Microbiol Rev* **32**:461–473. doi:10.1111/j.1574-
651 6976.2008.00101.x
652 Larabi A, Devos JM, Ng SL, Nanao MH, Round A, Maniatis T, Panne D. 2013. Crystal structure
653 and mechanism of activation of TANK-binding kinase 1. *Cell Rep* **3**:734–46.
654 doi:10.1016/j.celrep.2013.01.034
655 Laub MT, Biondi EG, Skerker JM. 2007. Phosphotransfer profiling: systematic mapping of
656 two-component signal transduction pathways and phosphorelays. *Methods Enzymol*
657 **423**:531–48. doi:10.1016/S0076-6879(07)23026-5
658 Laub MT, Goulian M. 2007. Specificity in two-component signal transduction pathways.
659 *Annu Rev Genet* **41**:121–45. doi:10.1146/annurev.genet.41.042007.170548
660 Lee KPK, Dey M, Neculai D, Cao C, Dever TE, Sicheri F. 2008. Structure of the dual enzyme
661 Ire1 reveals the basis for catalysis and regulation in non-conventional RNA splicing.
662 *Cell* **132**:89–100. doi:10.1016/j.cell.2007.10.057
663 Lin YC, Brown K, Siebenlist U. 1995. Activation of NF-kappa B requires proteolysis of the
664 inhibitor I kappa B-alpha: signal-induced phosphorylation of I kappa B-alpha alone
665 does not release active NF-kappa B. *Proceedings of the National Academy of Sciences*
666 **92**:552–556. doi:10.1073/pnas.92.2.552
667 Liu F, Xia Y, Parker AS, Verma IM. 2012. IKK biology. *Immunol Rev* **246**:239–53.
668 doi:10.1111/j.1600-065X.2012.01107.x
669 Liu S, Misquitta YR, Olland A, Johnson MA, Kelleher KS, Kriz R, Lin LL, Stahl M, Mosyak L.
670 2013. Crystal Structure of a Human IκB Kinase β Asymmetric Dimer. *J Biol Chem*
671 **288**:22758–22767. doi:10.1074/jbc.M113.482596
672 Lochhead PA. 2009. Protein kinase activation loop autophosphorylation in cis: overcoming a
673 Catch-22 situation. *Sci Signal* **2**:pe4. doi:10.1126/scisignal.254pe4
674 Lochhead PA, Kinstrie R, Sibbet G, Rawjee T, Morrice N, Cleghon V. 2006. A chaperone-
675 dependent GSK3beta transitional intermediate mediates activation-loop
676 autophosphorylation. *Mol Cell* **24**:627–633. doi:10.1016/j.molcel.2006.10.009
677 Lochhead PA, Sibbet G, Morrice N, Cleghon V. 2005. Activation-loop autophosphorylation is
678 mediated by a novel transitional intermediate form of DYRKs. *Cell* **121**:925–936.
679 doi:10.1016/j.cell.2005.03.034
680 Meyer AN, Drafahl KA, McAndrew CW, Gilda JE, Gallo LH, Haas M, Brill LM, Donoghue DJ.
681 2013. Tyrosine Phosphorylation Allows Integration of Multiple Signaling Inputs by
682 IKKβ. *PLoS One* **8**:e84497. doi:10.1371/journal.pone.0084497
683 Mooster JL, Le Bras S, Massaad MJ, Jabara H, Yoon J, Galand C, Heesters BA, Burton OT,
684 Mattoo H, Manis J, Geha RS. 2015. Defective lymphoid organogenesis underlies the
685 immune deficiency caused by a heterozygous S32I mutation in IκBα. *J Exp Med*
686 **212**:185–202. doi:10.1084/jem.20140979
687 Nolen B, Taylor S, Ghosh G. 2004. Regulation of Protein Kinases: Controlling Activity through
688 Activation Segment Conformation. *Molecular Cell* **15**:661–675.
689 doi:10.1016/j.molcel.2004.08.024

690 Otero JE, Dai S, Foglia D, Alhawagri M, Vacher J, Pasparakis M, Abu-Amer Y. 2008. Defective
691 osteoclastogenesis by IKKbeta-null precursors is a result of receptor activator of NF-
692 kappaB ligand (RANKL)-induced JNK-dependent apoptosis and impaired
693 differentiation. *J Biol Chem* **283**:24546–24553. doi:10.1074/jbc.M800434200
694 Polley S, Huang D-B, Hauenstein AV, Fusco AJ, Zhong X, Vu D, Schröfelbauer B, Kim Y,
695 Hoffmann A, Verma IM, Ghosh G, Huxford T. 2013. A structural basis for IκB kinase 2
696 activation via oligomerization-dependent trans auto-phosphorylation. *PLoS Biol*
697 **11**:e1001581. doi:10.1371/journal.pbio.1001581
698 Rieke C, Papendieck A, Sokolova O, Naumann M. 2011. Helicobacter pylori-induced tyrosine
699 phosphorylation of IKKβ contributes to NF-κB activation. *Biol Chem* **392**:387–393.
700 doi:10.1515/BC.2011.029
701 Robbins DJ, Zhen E, Owaki H, Vanderbilt CA, Ebert D, Geppert TD, Cobb MH. 1993.
702 Regulation and properties of extracellular signal-regulated protein kinases 1 and 2 in
703 vitro. *J Biol Chem* **268**:5097–106.
704 Rothwarf DM, Zandi E, Natoli G, Karin M. 1998. IKK-gamma is an essential regulatory subunit
705 of the IkappaB kinase complex. *Nature* **395**:297–300. doi:10.1038/26261
706 Sang D, Shu T, Pantoja CF, Ibáñez de Opakua A, Zweckstetter M, Holt LJ. 2022. Condensed-
707 phase signaling can expand kinase specificity and respond to macromolecular
708 crowding. *Mol Cell* **82**:3693-3711.e10. doi:10.1016/j.molcel.2022.08.016
709 Scheidereit C. 2006. IkappaB kinase complexes: gateways to NF-kappaB activation and
710 transcription. *Oncogene* **25**:6685–705. doi:10.1038/sj.onc.1209934
711 Schrofelbauer B, Hoffmann A. 2011. How do pleiotropic kinase hubs mediate specific
712 signaling by TNFR superfamily members? *Immunol Rev* **244**:29–43.
713 doi:10.1111/j.1600-065X.2011.01060.x
714 Schröfelbauer B, Polley S, Behar M, Ghosh G, Hoffmann A. 2012. NEMO ensures signaling
715 specificity of the pleiotropic IKKβ by directing its kinase activity toward IκBα. *Mol Cell*
716 **47**:111–121. doi:10.1016/j.molcel.2012.04.020
717 Shaul JD, Farina A, Huxford T. 2008. The human IKKbeta subunit kinase domain displays CK2-
718 like phosphorylation specificity. *Biochem Biophys Res Commun* **374**:592–7.
719 doi:10.1016/j.bbrc.2008.07.082
720 Sidrauski C, Walter P. 1997. The transmembrane kinase Ire1p is a site-specific endonuclease
721 that initiates mRNA splicing in the unfolded protein response. *Cell* **90**:1031–1039.
722 doi:10.1016/s0092-8674(00)80369-4
723 Stephenson AA, Taggart DJ, Xu G, Fowler JD, Wu H, Suo Z. 2022. The inhibitor of κB kinase β
724 (IKKβ) phosphorylates IκBα twice in a single binding event through a sequential
725 mechanism. *J Biol Chem* **299**:102796. doi:10.1016/j.jbc.2022.102796
726 Sugiyama N, Imamura H, Ishihama Y. 2019. Large-scale Discovery of Substrates of the
727 Human Kinome. *Sci Rep* **9**:10503. doi:10.1038/s41598-019-46385-4
728 Tergaonkar V, Bottero V, Ikawa M, Li Q, Verma IM. 2003. IkappaB kinase-independent
729 IkappaBalpha degradation pathway: functional NF-kappaB activity and implications
730 for cancer therapy. *Mol Cell Biol* **23**:8070–83.
731 Tigno-Aranjuez JT, Asara JM, Abbott DW. 2010. Inhibition of RIP2's tyrosine kinase activity
732 limits NOD2-driven cytokine responses. *Genes Dev* **24**:2666–2677.
733 doi:10.1101/gad.1964410
734 Tu D, Zhu Z, Zhou AY, Yun CH, Lee KE, Toms AV, Li Y, Dunn GP, Chan E, Thai T, Yang S, Ficarro
735 SB, Marto JA, Jeon H, Hahn WC, Barbie DA, Eck MJ. 2013. Structure and

736 ubiquitination-dependent activation of TANK-binding kinase 1. *Cell Rep* **3**:747–58.
737 doi:10.1016/j.celrep.2013.01.033
738 Xu G, Lo Y-C, Li Q, Napolitano G, Wu X, Jiang X, Dreano M, Karin M, Wu H. 2011. Crystal
739 structure of inhibitor of κB kinase β (IKKβ). *Nature* **472**:325–330.
740 doi:10.1038/nature09853
741 Ye Q, Crawley SW, Yang Y, Côté GP, Jia Z. 2010. Crystal structure of the alpha-kinase domain
742 of Dictyostelium myosin heavy chain kinase A. *Sci Signal* **3**:ra17.
743 doi:10.1126/scisignal.2000525
744 Zandi E, Chen Y, Karin M. 1998. Direct phosphorylation of IkappaB by IKKalpha and IKKbeta:
745 discrimination between free and NF-kappaB-bound substrate. *Science* **281**:1360–
746 1363. doi:10.1126/science.281.5381.1360
747 Zandi E, Rothwarf DM, Delhase M, Hayakawa M, Karin M. 1997. The IkappaB kinase complex
748 (IKK) contains two kinase subunits, IKKalpha and IKKbeta, necessary for IkappaB
749 phosphorylation and NF-kappaB activation. *Cell* **91**:243–252. doi:10.1016/s0092-
750 8674(00)80406-7
751 Zhang J, Clark K, Lawrence T, Peggie MW, Cohen P. 2014. An unexpected twist to the
752 activation of IKKbeta: TAK1 primes IKKbeta for activation by autophosphorylation.
753 *Biochem J* **461**:531–7. doi:10.1042/BJ20140444
754

755

756

757

Figure legends:

Figure 1: Autophosphorylation of IKK2 at hitherto uncharacterized sites. (A) A schematic of the IKK-complex (pre- and post-stimulation) showing binding of NEMO helping activation of IKK as well as channelizing its recognition of substrate IκBα. The mechanism of specific phosphorylation at Ser32 and Ser36 of IκBα is unclear **(B)** Domain organization of IKK2 based on the X-ray structures highlighting its functional kinase domain (KD), ubiquitin-like domain (ULD), scaffold dimerization domain (SDD), and NEMO-binding domain. Serine residues in the activation loop - substitution of which to glutamate renders IKK2 constitutively active and those in the SRR region known to be phosphorylated are marked. Tyrosine residues in the activation loop and the conserved ATP-interacting Lys44 are also marked. **(C)** *In vitro* kinase assay showing autophosphorylation of wild-type full-length IKK2 (FL IKK2WT) upon incubation with γ^{32}P radiolabeled ATP for different time periods. **(D)** Similar *in vitro* kinase assays performed to assess the effect of NEMO on autophosphorylation of FL IKK2WT (left panel), and the effect of NEMO and IκBα on autophosphorylation and substrate phosphorylation (right panel) activities of FL IKK2WT. **(E)** *In vitro* kinase assay (schematic depicted in Figure S1B) showing effect of different concentrations of the Inhibitor VII on FL IKK2WT autophosphorylation and IκBα substrate phosphorylation (this assay was performed twice). **(F)** Kinase assay with radiolabeled ATP displaying auto- and substrate-phosphorylation of full-length and deletion constructs of the constitutively active form of IKK2 harbouring phosphomimetic Ser177Glu and Ser181Glu substitutions.

Figure 2: IKK2 displays autocatalytic dual specificity. (A) *In vitro* kinase assay with unlabeled ATP showing autophosphorylations in FL IKK2WT detected by immunoblotting using antibodies specific against phosphor-Ser (177/181) and phospho-Tyr residues. **(B)** pTyr on IKK2 detected using a different commercial source of phospho-Tyr antibody. **(C)** Effect of Inhibitor VII on tyrosine autophosphorylation of FL IKK2WT. **(D)** Autophosphorylation of IKK2 K44M mutant compared to that of IKK2 WT assessed at different time points through immunoblotting performed with phospho-Tyr antibody. **(E)** Autophosphorylation of tyrosines along with phosphorylation of GST-tagged IκBα (1-54) substrate with full-length and deletion mutants of IKK2 harbouring phosphomimetic Ser177Glu and Ser181Glu substitutions. **(F)** *In vitro De novo* auto-phosphorylation of IKK2 Δ664EE construct on tyrosine analysed by phospho-Ser and phospho-Tyr specific monoclonal antibodies. **(G)** Autophosphorylations at tyrosine and AL-serine residues upon fresh ATP-treatment of FLIKK2 WT and FLIKK2 S177A,S181A assessed by immunoblot analysis using antibodies against phospho-IKK2-Ser(177/181) and phospho-Tyr.

Figure 3: Dual-specific autophosphorylation is critical for function of IKK2: (A) A surface representation of IKK2-KD structure (adapted from PDB ID 4E3C; KD is shown in light green and SDD in teal) with positions of canonically important residues within the AL (purple ribbon) marked. Tyrosine residues in the activation segment are marked in green, Tyr169 among which is identified to be autophosphorylated. **(B)** Amino-acid sequence alignment of activation loop segment of different kinases in the IKK-family. The tyrosine at position DFG+1 (DLG+1 in case of IKK1 and IKK2) is observed only in IKK and in the stress response related plant kinase SnRK2, but not in other structural homologues of IKK or dual specificity kinases, e.g., DYRK and GSK3β (both contain Ser at that position). Tyr at position 188 (204 in PKA) is universally conserved. **(C)** Substrate and autophosphorylation activities of FL IKK2 WT and IKK2 K44M mutant were compared using *in vitro* radioactive kinase assay in presence and absence of FL IκBα WT as the substrate. **(D)** Specific residue-selectivity of phosphorylation by the FL IKK2 K44M analysed using an antibody specific for phospho-S32/36 of IκBα. **(E)** *In vitro* kinase assay using radiolabeled ATP performed with IKK2 WT and IKK2 Y169F in presence of WT and AA-mutant of GST-tagged IκBα (1-54) substrate. **(F)** *In vitro* kinase assay using radiolabeled ATP performed with IKK2 Y169F mutant in presence of various GST-tagged IκBα(1-54) substrates indicating abolition of substrate phosphorylation in S36A and S36E mutants of IκBα. **(G)** Severe reduction of IKK activity with IKK immunoprecipitated (IP-ed) with anti-NEMO antibody from whole cell extract (n=2) of TNFα-induced *ikk2*$^{-/-}$ MEF-3T3 cells reconstituted with mutant Y169F IKK2 compared to the wild-type.

Figure 4: Structural analyses of IKK2 autophosphorylation. Figure 4: Structural analyses of IKK2 autophosphorylation. (A) Molecular dynamics (MD) simulations of three differently phosphorylated states of IKK2 - UnP-IKK2, p-IKK2, and P-IKK2, and 200ns trajectory of energy of these states shown in golden yellow, blue, and copper red, respectively. Same coloring scheme has been maintained in this figure and in the corresponding supplementary figure (see Supplementary file 3 for additional details). **(B)** 200ns trajectory of RMSD of the three states (see Supplementary file 4 for additional details). **(C)** Superposition of structures representing the differently phosphorylated states post 200ns MD simulation. Relevant regions, e.g., activation loop, αC-helix, Gly-rich loop areas are highlighted in the right panel. **(D)** Residues forming canonical R- (labelled in blue) and C-spines (labelled in dark gray) representing an active conformation in p-IKK2 are shown. **(E)** ATP-bound p-IKK2 structure is depicted. In the right panel, relevant residues are

highlighted. The position of Tyr169 is conducive to autophosphorylation. **(F)** ATP maintains the desired continuum of R- and C-spines observed in active kinase conformations. **(G)** P-IKK2 cannot accommodate ATP in its cleft, and αC-helix is displaced. **(H)** Met65 is moved away from the R-spine, failing to form canonically active conformation of R- and C-spines. **(I & J)** ADP-bound states of p-IKK2 and P-IKK2, both of which can accommodate ADP in their respective clefts.

Figure 5: Freshly autophosphorylated IKK2 relays phosphates to IκBα. (A) A schematic of the autoradiography experiment to monitor path of phosphate(s) from phospho-IKK2 to substrate. **(B)** Autophosphorylated (with radiolabeled ATP) purified IKK2 could transfer its phosphate to IκBα substrate in absence of any nucleotide, and the transfer efficiency is enhanced upon addition of ADP or ATP. **(C)** A schematic of the immunoblot experiment to monitor path of phosphate(s) from phospho-IKK2 to substrate. **(D)** Elution profile in size-exclusion chromatography (Superdex200 10/30 increase) of phospho-IKK2 (Peak 1) to remove excess unlabeled ATP (Peak 2). Phospho-IKK2 from Peak1 was used in downstream phosphotransfer assays. **(E)** Immunoblotting experiment using specific antibodies indicated in the figure showing that purified autophosphorylated (with cold ATP) IKK2 transfers its phosphate to IκBα substrate and this transfer efficiency is enhanced upon addition of ADP or ATP (n=2).

Figure 6: Specificity and fidelity of phosphotransfer by IKK2 to IκBα. (**A**) Autoradiograph showing phosphotransfer to full-length IκBα WT but not to its S32A,S36A double mutant. Domain organization and position of relevant S/T/Y residues of IκBα are shown above the autoradiograph. Also, AMP-PNP can support efficient phosphotransfer. **(B)** A proposed scheme of reactions during signal-responsive IKK2-activation and subsequent specific phosphorylation of IκBα at S32,S36 through phosphotransfer in presence of ADP.

Figure 1 - figure supplement 1: (A) Autoradiograph of an *in vitro* kinase assay showing auto- and substrate-phosphorylations with FL IKK2WT or IKK2 K44M using substrate GST-tagged IκBα (1-54) as a function of time. **(B)** *In vitro* kinase assay with cold ATP showing effect of different Inhibitor VII concentrations on substrate phosphorylation activity of FL IKK2 WT. FL IκBα WT was used as the substrate and phosphorylation specifically at S32/S36 was monitored using a monoclonal antibody specific for IκBα phosphorylated at those two serines. A scheme of the kinase assay is shown below. **(C)** Coomassie-stained SDS-PAGE gel showing general purity of the IKK2 proteins (WT and K44M) used in this study (Left panel). Silver-stained SDS-PAGE gel showing purity of 3 different FL IKK2

protein constructs (WT, Y169F and K44M) used in the study. **(D)** LC MS/MS analyses of FL IKK2 K44M protein after Trypsin digestion on Orbitrap Exploris^{TM} 240 equipment. A 3D scatter plot with different parameters for the detected proteins obtained from the mass spectrometric analysis of the sample is shown, where X-axis represents number of unique peptides for each protein, Y-axis represents spectral counts, and Z-axis represents the iBAQ (intensity Based Absolute Quantification) values. KyPlot was used to create this 3D scatter plot. In the left panel all the proteins detected are shown where orange circle represents the protein kinases, whereas in the right panel only the protein kinases are shown for better clarity. For this analysis *Spodoptera frugiperda* reference proteome (ID: UP000829999) available in Uniprot database was used that contains both reviewed (Swiss-Prot) and unreviewed (TrEMBL) protein sequences.

Figure 2 – figure supplement 1: (A) *In vitro* kinase assay monitored by immunoblotting showing the effect of increasing concentration of urea on tyrosine autophosphorylation of FL IKK2WT. **(B)** *In vitro* kinase assay using radiolabeled ATP to test auto- and substrate-phosphorylations with up to 6M urea. **(C)** Effects of common kinase inhibitors e.g., AMPPNP and Staurosporine, highly specific IKK2 inhibitors TPCA, Calbiochem Inhibitor VII and MLN120B on inhibition of both substrate phosphorylation and tyrosine autophosphorylation activities of IKK2. Immunoblotting using specific antibodies as indicated in the figure were used to monitor the phosphorylation and protein levels. **(D)** *In vitro* kinase assay showing substitution of AL-serines to non-phosphorylatable alanine (FL IKK2 S177A,181A double mutant) debilitates kinase activity of IKK2 towards S32,S36 of IκBα compared to its WT version.

Figure 3 – figure supplement 1: (A) LC-MS/MS based detection of phosphorylated tyrosine residue, Y169) on autophosphorylated FL IKK2 WT. **(B)** A close-up view of the active site in active form in the context of the entire kinase domain of IKK2. Three tyrosines (Y169, Y188 and Y199) in immediate vicinity of active sites are highlighted. Position of ATP is modelled based on the ATP-bound structure of PKA. **(C)** Substrate bound PKA in its active form; phosphorylatable serine of the substrate peptide (in magenta) is highlighted. **(D)** Immunoblotting performed with phospho-IKK2 S177/S181 antibody to check autophosphorylation in IKK2 K44M mutant at different time points compared to that of IKK2 WT. **(E)** Differential sensitivity of specific vs. non-specific phosphorylation by IKK2 displayed in the effect of Inhibitor VII on FL IKK2 WT and IKK2 K44M in presence of either IκBα WT or IκBα AA as substrates. **(F)** To compare IKK2 Y169F to IKK2 WT for phosphorylation of S32 and S36 of IκBα, assay similar to that described in Figure 3F was performed. Reactions with

IKK2 WT and IKK2 Y169F were run on different gels but the gels were similarly processed and exposed for autoradiography before imaging (n=1). **(G)** AL-serine phosphorylation status of immunoprecipitated [with monoclonal anti-HA antibody (n=2)] IKK2 WT and IKK2 Y169F from TNF-α-stimulated reconstituted MEF cells.

Figure 4 – figure supplement 1: (A) A differential scanning calorimetry (DSC) thermogram showing a striking enhancement in folding stability of IKK2 upon ATP-treatment (n=1). **(B)** Ribbon representation of different phosphorylated versions of IKK2 are shown: UnP-IKK2 in golden yellow, p-IKK2 in blue and P-IKK2 in copper red. **(C)** Trajectories of RMSF for these structures are shown (left panel). For clarity, different regions of the KD are shown in the right panel. **(D)** Dynamic cross-correlation matrix (DCCM) or contact map of each structure reveals phosphorylation-induced local as well as allosteric changes. **(E)** Docking scores of ATP and ADP bound differently phosphorylated IKK2 proteins using three different docking programs. ATP and ADP were docked to respective IKK2 models at 0ns and at 200ns using LeDock and GOLD followed by rescoring with AutoDock Vina (see methods). **(F)** Percentage of unfavorable poses having $\Delta G>0$ obtained from MM-PBSA (Molecular Mechanics Poisson-Boltzmann Surface Area) method for each phosphorylated state of IKK2 using 50 intermediate complex structures in a 10ns MD simulation of respective complex structures post-docking (see methods). **(G)** ATP-bound structure of p-IKK2 (ribbon) is shown.

Figure 5 – figure supplement 1: (A) Quantitation of phospho-IκBα (at S32/S36) and tyrosine phosphorylated IKK2 described in Figure 5E using ImageQuant TL software. The average intensity values were obtained upon subtracting the background noise, and the ratios of the average intensity of the phosphorylated protein with respect to the intensity of total protein were plotted using Microsoft Excel. **(B)** Transfer of phosphates from purified autophosphorylated (unlabeled ATP) IKK2 to IκBα substrate increases in presence of a fixed concentration of ADP in a time-dependent manner. Progress of the reaction is monitored by immunoblotting using specific antibodies as indicated in the figure (n=2). **(C)** ESI-MS scan of the ADP used in this assay system showing negligible trace, if any, of ATP at 50 μM ADP concentration. **(D)** Regeneration of ATP, if any, through microscopic reversibility was checked by TLC in a variety of conditions. γ-P^{32} was used as the control/standard.

Figure 6 – figure supplement 1: Purified autophosphorylated (radiolabeled) FL IKK2 Y169F fails to transfer phosphate to IκBα substrate in absence or presence of ADP (n=1). This assay was performed similarly to that described in Figure 5A.

Figure 1

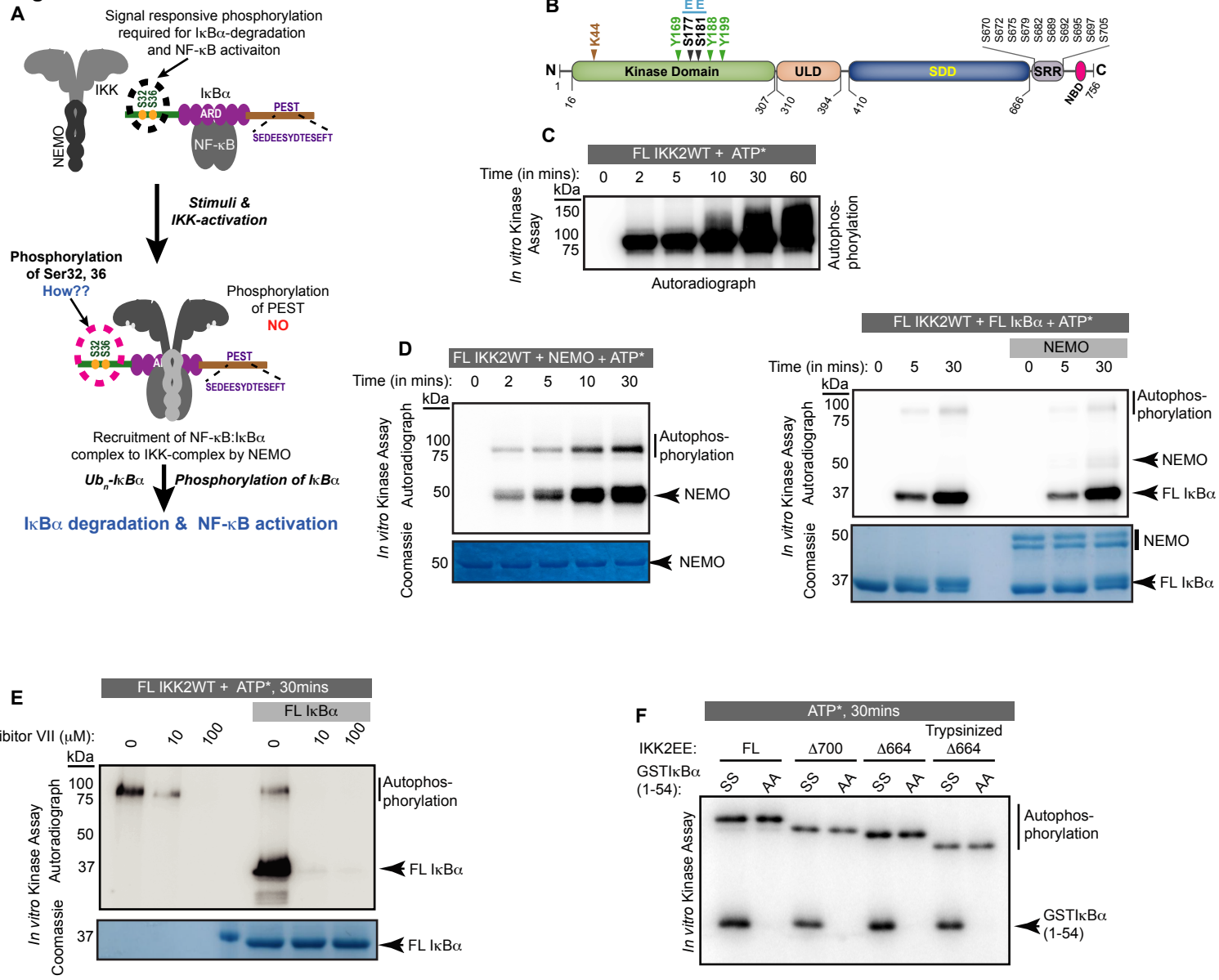
A
Signal responsive phosphorylation required for IκBα-degradation and NF-κB activaiton
IKK
NEMO
S32
S36
IκBα
ARD
PEST
SEDEESYDTESEFT
NF-κB
Stimuli & IKK-activation
Phosphorylation of Ser32, 36
How??
Phosphorylation of PEST
NO
Recruitment of NF-κB:IκBα complex to IKK-complex by NEMO
Ubn-IκBα
Phosphorylation of IκBα
IκBα degradation & NF-κB activation
B
Constitutively Active
E E
K44
Y169
S177
S181
Y188
Y199
S670
S672
S675
S679
S682
S689
S692
S695
S697
S705
N
Kinase Domain
ULD
SDD
SRR
C
NBD
1
16
307
310
394
410
666
756
C
FL IKK2WT + ATP*
Time (in mins): 0 2 5 10 30 60
kDa
150
100
75
In vitro Kinase Assay
Autoradiograph
Autophos-phorylation
D
FL IKK2WT + NEMO + ATP*
Time (in mins): 0 2 5 10 30
kDa
100
75
50
Autophos-phorylation
NEMO
Coomassie
50
NEMO
FL IKK2WT + FL IκBα + ATP*
NEMO
Time (in mins): 0 5 30 0 5 30
kDa
100
75
50
37
Autophos-phorylation
NEMO
FL IκBα
Coomassie
50
37
NEMO
FL IκBα
E
FL IKK2WT + ATP*, 30mins
FL IκBα
Inhibitor VII (μM): 0 10 100 0 10 100
kDa
100
75
50
37
Autophos-phorylation
FL IκBα
Coomassie
37
FL IκBα
F
ATP*, 30mins
IKK2EE: FL Δ700 Δ664 Trypsinized Δ664
GSTIκBα (1-54): SS AA SS AA SS AA SS AA
Autophos-phorylation
GSTIκBα (1-54)

Figure 2

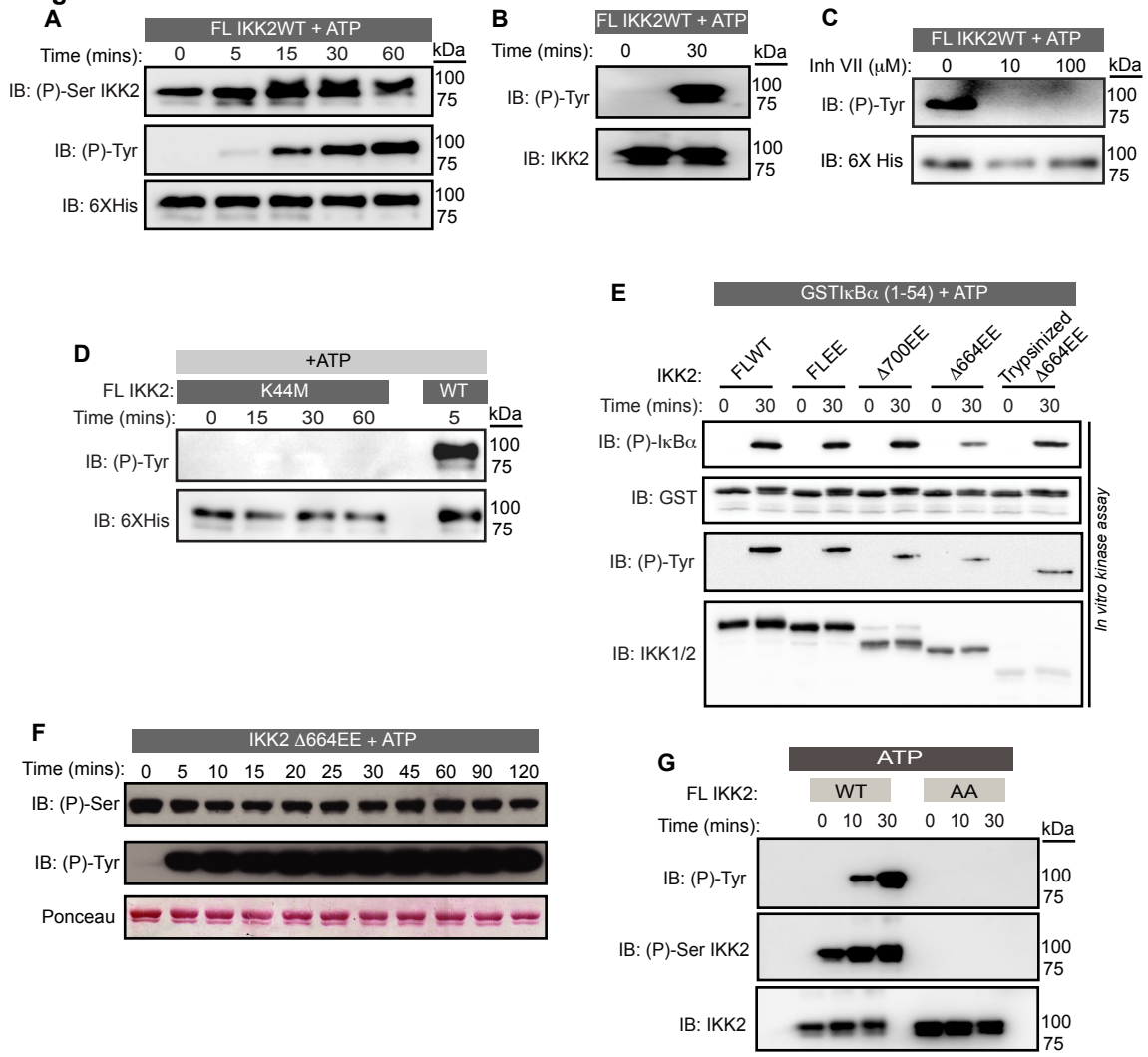
A
FL IKK2WT + ATP
Time (mins): 0 5 15 30 60
kDa
IB: (P)-Ser IKK2
IB: (P)-Tyr
IB: 6XHis
100
75
B
FL IKK2WT + ATP
Time (mins): 0 30
kDa
IB: (P)-Tyr
IB: IKK2
C
FL IKK2WT + ATP
Inh VII (μM): 0 10 100
kDa
IB: (P)-Tyr
IB: 6X His
D
+ATP
FL IKK2: K44M WT
Time (mins): 0 15 30 60 5
kDa
IB: (P)-Tyr
IB: 6XHis
E
GSTIκBα (1-54) + ATP
IKK2: FLWT FLEE Δ700EE Δ664EE Trypsinized Δ664EE
Time (mins): 0 30 0 30 0 30 0 30 0 30
IB: (P)-IκBα
IB: GST
IB: (P)-Tyr
IB: IKK1/2
In vitro kinase assay
F
IKK2 Δ664EE + ATP
Time (mins): 0 5 10 15 20 25 30 45 60 90 120
IB: (P)-Ser
IB: (P)-Tyr
Ponceau
G
ATP
FL IKK2: WT AA
Time (mins): 0 10 30 0 10 30
kDa
IB: (P)-Tyr
IB: (P)-Ser IKK2
IB: IKK2

Figure 3

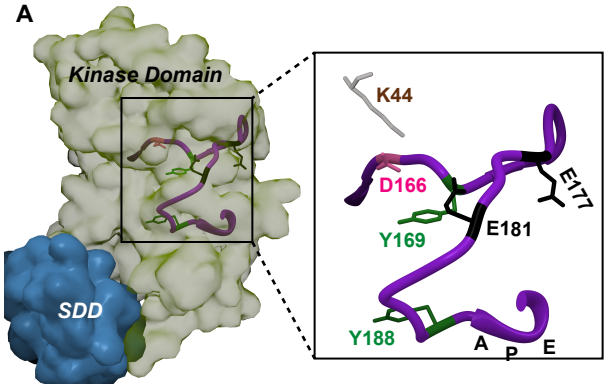
A
Kinase Domain
SDD
K44
D166
Y169
E181
E177
Y188
A
P
E

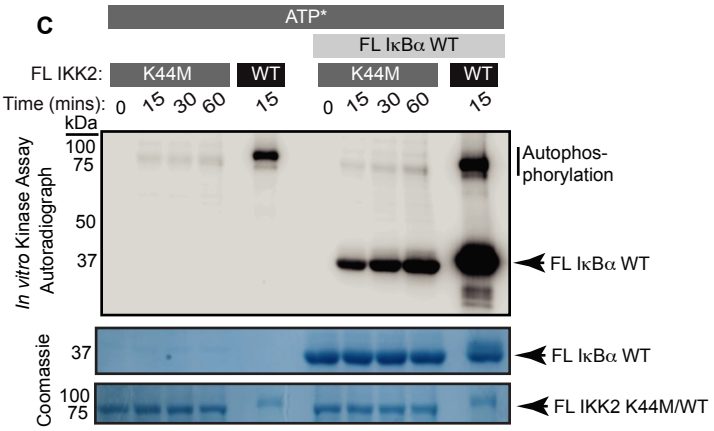
C
ATP*
FL IκBα WT
FL IKK2:
K44M
WT
K44M
WT
Time (mins):
0 15 30 60 15
0 15 30 60 15
kDa
100
75
50
37
In vitro Kinase Assay Autoradiograph
Autophos-phorylation
FL IκBα WT
Coomassie
37
FL IκBα WT
100
75
FL IKK2 K44M/WT

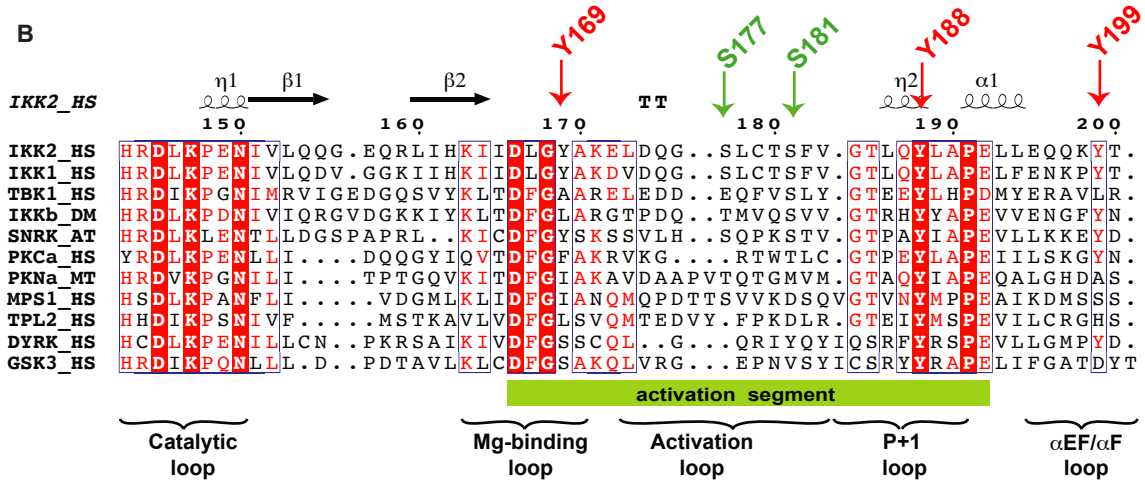
B
IKK2_HS
η1
β1
β2
Y169
TT
S177
S181
η2
Y188
α1
Y199
150
160
170
180
190
200
IKK2_HS HRDLKPENIVLQQG.EQRLIHKIIDLGYAKELDQG..SLCTSFV.GTLQYLAPELLEQQKYT.
IKK1_HS HRDLKPENIVLQDV.GGKIIHKIIDLGYAKDVDQG..SLCTSFV.GTLQYLAPELFENKPYT.
TBK1_HS HRDIKPGNIMRVIGEDGQSVYKLTDFGAARELEDD..EQFVSLY.GTEEYLHPDMYERAVLR.
IKKb_DM HRDLKPDNIVIQRGVDGKKIYKLTDFGLARGTPDQ..TMVQSVV.GTRHYYAPEVVENGFYN.
SNRK_AT HRDLKLENTLLDGSPAPRL..KICDFGYSKSSVLH..SQPKSTV.GTPAYIAPEVLLKKEYD.
PKCa_HS YRDLKPENLLI....DQQGYIQVTDFGFAKRVKG....RTWTLC.GTPEYLAPEIILSKGYN.
PKNa_MT HRDVKPGNILI....TPTGQVKITDFGIAKAVDAAPVTQTGMVM.GTAQYIAPEQALGHDAS.
MPS1_HS HSDLKPANFLI.....VDGMLKLIDFGIANQMQPDTTSVVKDSQVGTVNYMPPEAIKDMSSS.
TPL2_HS HHDIKPSNIVF.....MSTKAVLVDFGLSVQMTEDVY.FPKDLR.GTEIYMSPEVILCRGHS.
DYRK_HS HCDLKPENILLCN..PKRSAIKIVDFGSSCQL..G...QRIYQYIQSRFYRSPEVLLGMPYD.
GSK3_HS HRDIKPQNLLL.D..PDTAVLKLCDFGSAKQLVRG...EPNVSYICSRYYRAPELIFGATDYT
activation segment
Catalytic loop
Mg-binding loop
Activation loop
P+1 loop
αEF/αF loop

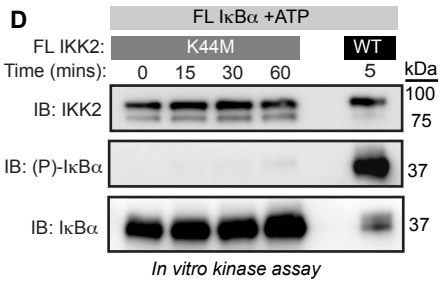
D
FL IκBα +ATP
FL IKK2:
K44M
WT
Time (mins):
0 15 30 60 5
kDa
IB: IKK2
100
75
IB: (P)-IκBα
37
IB: IκBα
37
In vitro kinase assay

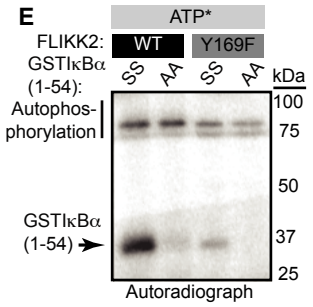
E
ATP*
FLIKK2:
WT
Y169F
GSTIκBα (1-54):
SS
AA
SS
AA
kDa
Autophos-phorylation
100
75
50
GSTIκBα (1-54)
37
25
Autoradiograph

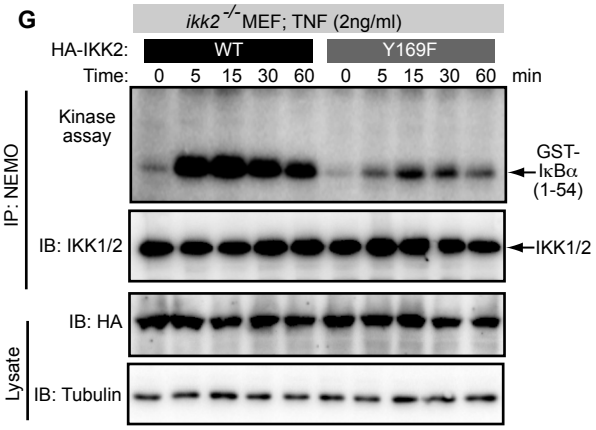
G
ikk2 -/- MEF; TNF (2ng/ml)
HA-IKK2:
WT
Y169F
Time:
0 5 15 30 60 0 5 15 30 60 min
IP: NEMO
Kinase assay
GST-IκBα (1-54)
IB: IKK1/2
IKK1/2
IB: HA
Lysate
IB: Tubulin

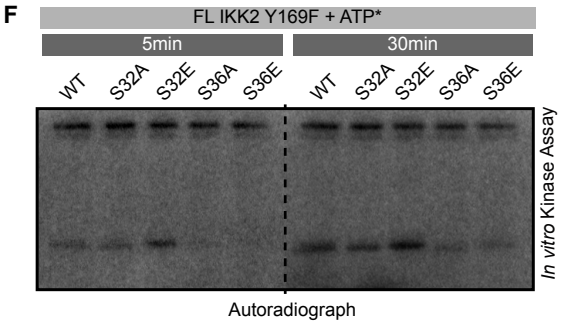
F
FL IKK2 Y169F + ATP*
5min
30min
WT
S32A
S32E
S36A
S36E
WT
S32A
S32E
S36A
S36E
In vitro Kinase Assay
Autoradiograph

Figure 4

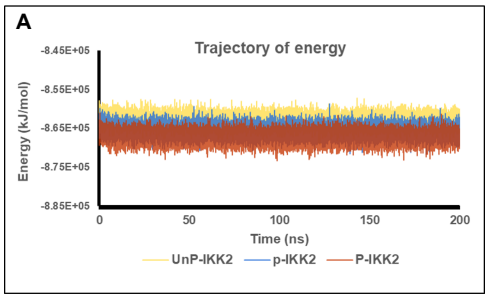
A
Trajectory of energy
Energy (kJ/mol)
-8.45E+05
-8.55E+05
-8.65E+05
-8.75E+05
-8.85E+05
0
50
100
150
200
Time (ns)
UnP-IKK2
p-IKK2
P-IKK2

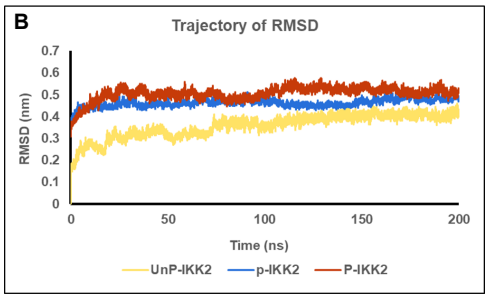
B
Trajectory of RMSD
RMSD (nm)
0.7
0.6
0.5
0.4
0.3
0.2
0.1
0
0
50
100
150
200
Time (ns)
UnP-IKK2
p-IKK2
P-IKK2

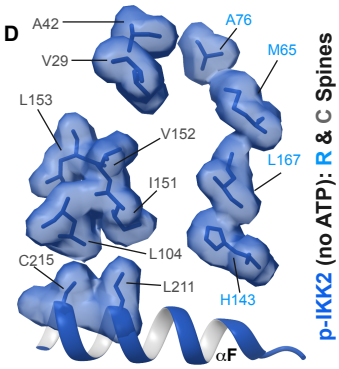
D
A42
V29
L153
A76
M65
V152
L167
I151
L104
C215
L211
H143
αF
p-IKK2 (no ATP): R & C Spines

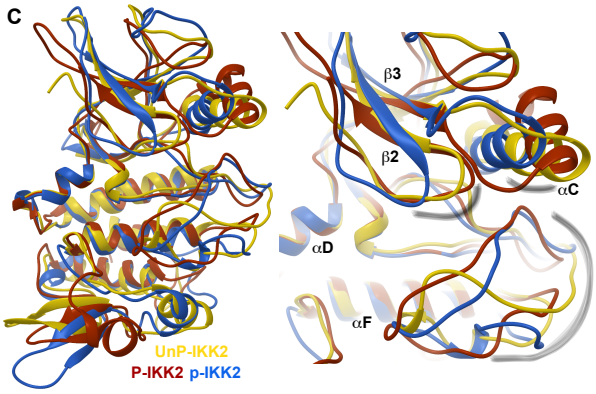
C
UnP-IKK2
P-IKK2 p-IKK2
β3
β2
αC
αD
αF

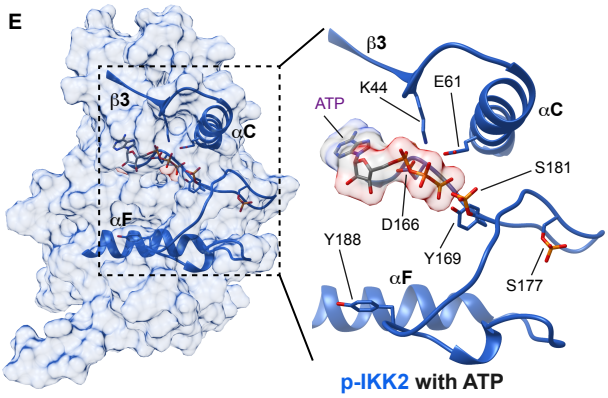
E
β3
αC
αF
β3
ATP
K44
E61
αC
S181
D166
Y188
Y169
αF
S177
p-IKK2 with ATP

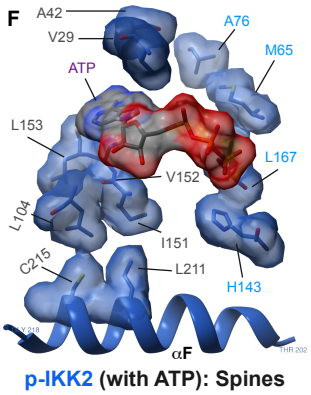
F
A42
V29
A76
M65
ATP
L153
L167
V152
L104
I151
C215
L211
H143
αF
p-IKK2 (with ATP): Spines

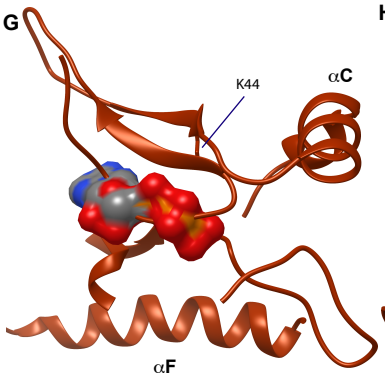
G
K44
αC
αF
P-IKK2:ATP

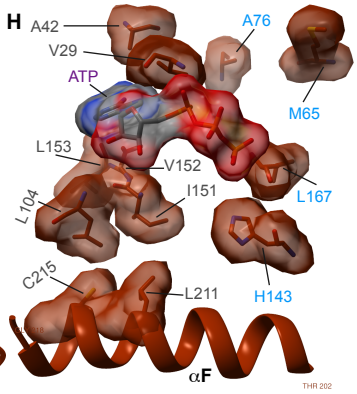
H
A42
V29
ATP
A76
M65
L153
V152
L167
L104
I151
C215
L211
H143
αF
P-IKK2 (with ATP): Spines

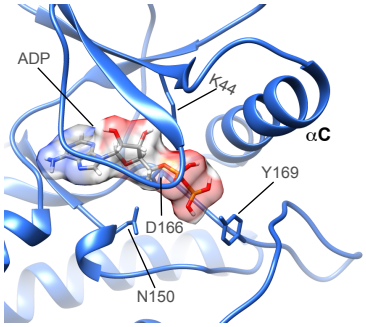
I
ADP
K44
αC
Y169
D166
N150
p-IKK2:ADP

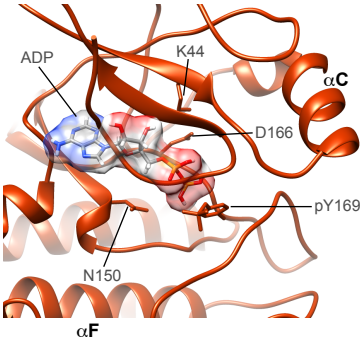
J
ADP
K44
αC
D166
pY169
N150
αF
P-IKK2:ADP

Figure 5

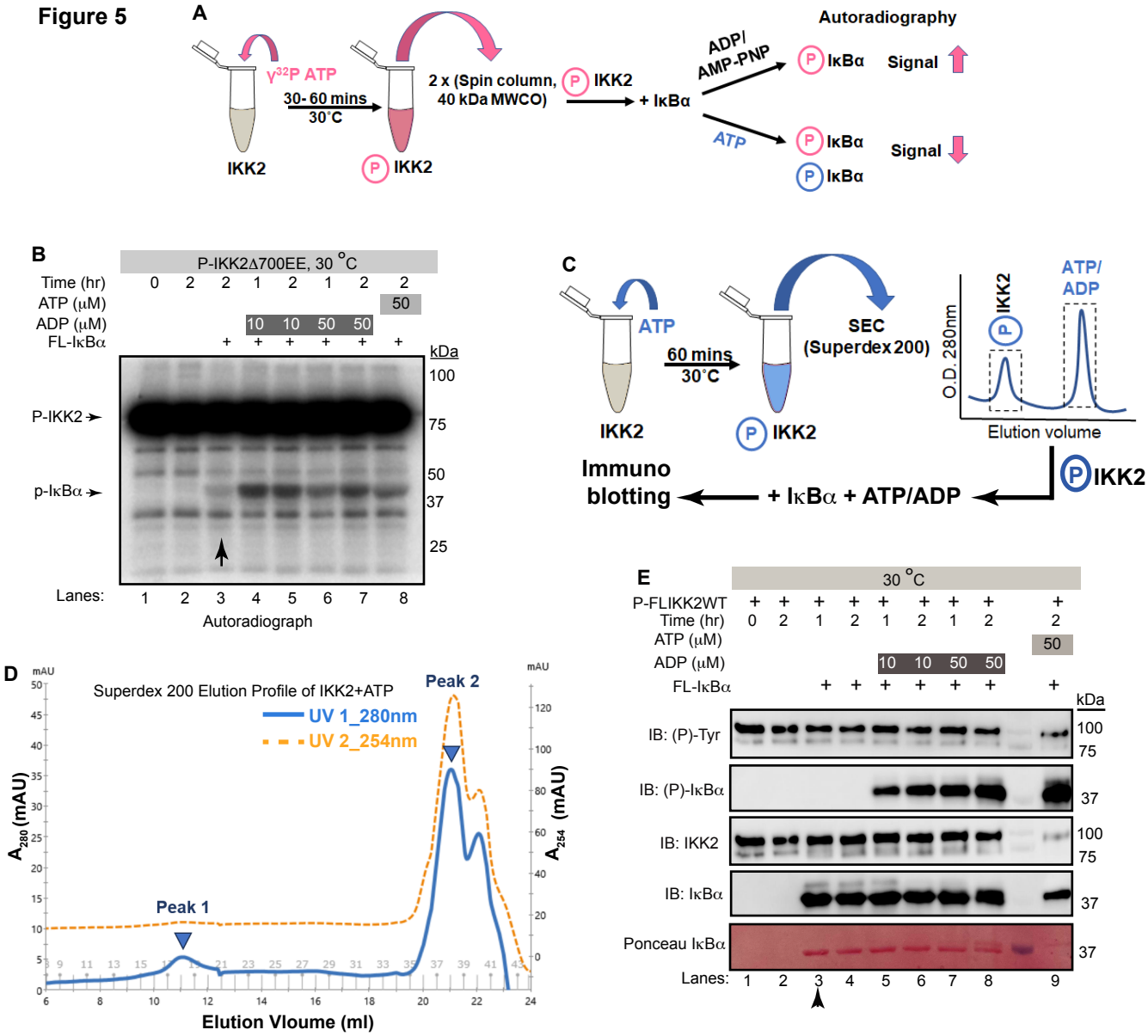
A
γ32P ATP
30- 60 mins
30°C
IKK2
P IKK2
2 x (Spin column, 40 kDa MWCO)
P IKK2
+ IκBα
ADP/ AMP-PNP
ATP
Autoradiography
P IκBα
Signal
P IκBα
P IκBα
Signal
B
P-IKK2Δ700EE, 30 °C
Time (hr) 0 2 2 1 2 1 2 2
ATP (μM) 50
ADP (μM) 10 10 50 50
FL-IκBα + + + + + +
kDa
100
75
50
37
25
P-IKK2
p-IκBα
Lanes: 1 2 3 4 5 6 7 8
Autoradiograph
C
ATP
60 mins
30°C
IKK2
P IKK2
SEC (Superdex 200)
O.D. 280nm
IKK2
ATP/ ADP
Elution volume
P IKK2
+ IκBα + ATP/ADP
Immuno blotting
D
Superdex 200 Elution Profile of IKK2+ATP
UV 1_280nm
UV 2_254nm
Peak 1
Peak 2
mAU
A280 (mAU)
A254 (mAU)
Elution Vloume (ml)
E
30 °C
P-FLIKK2WT + + + + + + + + +
Time (hr) 0 2 1 2 1 2 1 2 2
ATP (μM) 50
ADP (μM) 10 10 50 50
FL-IκBα + + + + + +
kDa
IB: (P)-Tyr
IB: (P)-IκBα
IB: IKK2
IB: IκBα
Ponceau IκBα
100
75
37
100
75
37
37
Lanes: 1 2 3 4 5 6 7 8 9

Figure 6

A

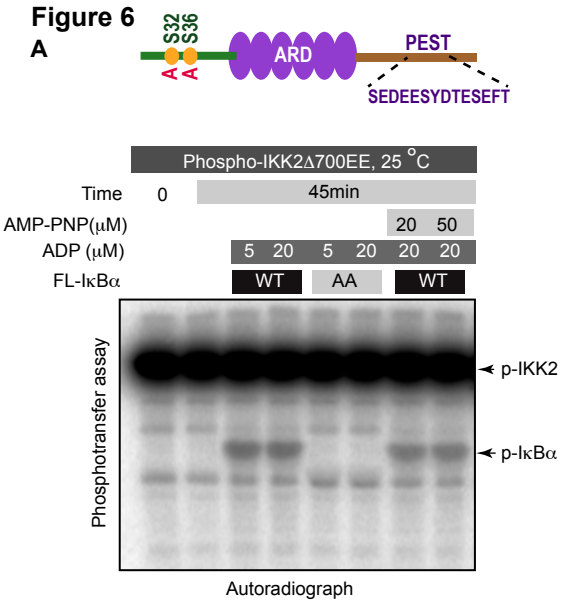
S32
S36
A
A
ARD
PEST
SEDEESYDTESEFT
Phospho-IKK2Δ700EE, 25 °C
Time
0
45min
AMP-PNP(μM)
20
50
ADP (μM)
5
20
5
20
20
20
FL-IκBα
WT
AA
WT
Phosphotransfer assay
p-IKK2
p-IκBα
Autoradiograph

B

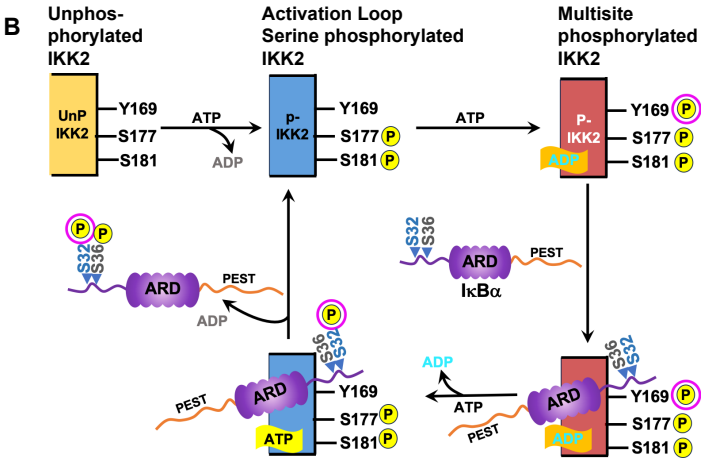
Unphos-
phorylated
IKK2
Activation Loop
Serine phosphorylated
IKK2
Multisite
phosphorylated
IKK2
UnP
IKK2
Y169
S177
S181
ATP
ADP
p-
IKK2
P-
IKK2
S32
S36
ARD
PEST
IκBα